이학석사 학위논문

WEE1 억제제의 항종양 효과와 DNA 손상 반응의 조절에 의한 PARP 억제제의 민감성 강화에 관한 연구

Antitumor effect of a WEE1 inhibitor and potentiation of PARP inhibitor sensitivity by modulation of DNA damage response

2018 년 8 월

서울대학교 대학원

의학대학 협동과정 종양생물학 전공

하 동 현

WEE1 억제제의 항종양 효과와 DNA 손상 반응의 조절에 의한 PARP 억제제의 민감성 강화에 관한 연구

지도교수 임 석 아

이 논문을 이학석사 학위논문으로 제출함.

2018년 4월

서울대학교 대학원

의학대학 협동과정 종양생물학 전공

하 동 현

하 동 현의 이학석사 학위논문을 인준함.

2018년 7월

위 원 장 _____ (인)

부위원장 _____ (인)

위 원 _____ (인)

Antitumor effect of a WEE1 inhibitor and potentiation of PARP inhibitor sensitivity by modulation of DNA damage response

By

Dong Hyeon Ha

(Directed by Seock-Ah Im, M.D., Ph.D.)

A Thesis Submitted to the Interdisciplinary Graduate Program in Partial Fulfillment of the Requirements for the Degree of Master of Philosophy in Cancer Biology at the Seoul National University, Seoul, Korea

July, 2018

Approved by thesis committee:

Professor _____ **Chairperson**

Professor _____ **Vice Chairperson**

Professor _____

ABSTRACT

Antitumor effect of a WEE1 inhibitor and potentiation of PARP inhibitor sensitivity by modulation of DNA damage response.

Dong Hyeon Ha

Major in Cancer Biology

Interdisciplinary Graduate Program

The Graduate School

Seoul National University

WEE1 plays an essential role in regulating the G2 / M checkpoint of the cell cycle by regulating CDK1 phosphorylation and is involved in stabilization and initiation of

a replication fork. WEE1 is also known that regulating the activity of target CDK1 is involved in DNA repair by regulating BRCA1 phosphorylation.

WEE1 inhibitor has been reported to increase the genomic instability by inducing DNA replication stress and the G2 / M checkpoint induced by DNA damage does not function, resulting in increased the cytotoxic effect of the DNA damage agents in various carcinomas.

This study aims to investigate the anti-tumor effect of WEE1 inhibitor, AZD1775 and the mechanism of increasing the sensitivity of PARP inhibitor by modulating homologous recombination repair in triple negative breast cancer cells.

AZD1775 induced caspase-3 dependent cell death in a sensitive MDA-MB-231 cell line and induced dysregulated cell cycle activation, such as accelerating S phase initiation and early mitotic entry. In addition, AZD1775 suppressed the expression

levels of proteins involved in the DNA damage repair response and inhibited the foci formation of RAD51. Thus AZD1775 led to the inhibition of homologous recombination repair, consequently prevented repair of damaged DNA. Thus, AZD1775 enhanced the cell sensitivity of the PARP inhibitor, olaparib, and this combination treatment improved the anti-tumor effect of AZD1775 and olaparib alone in the *in vivo* xenograft model of MDA-MB-231 cell line by compromising homologous recombination repair.

The results of this study suggest that combination therapy of AZD1775 alone or olaparib in triple negative breast cancer suggests the possibility of the anticancer effect and supports the rationale for clinical trial of combination therapy of olaparib and AZD1775.

Abberviation : HR, Homologous recombination repair; HRD, homologous

recombination repair deficiency; PARP, poly (ADP-ribose)polymerase,

Keywords: WEE1 inhibitor, PARP inhibitor, homologous recombination repair, combination therapy, triple negative breast cancer

***Student Number*: 2016-23104**

TABLE OF CONTENTS

LIST OF TABLES

LIST OF FIGURES

Introduction

Triple negative breast cancer (TNBC) is a breast cancer subtype that lacks estrogen receptor (ER) and progesterone receptor (PR) expression and does not show amplification of human epidermal growth factor receptor 2 (HER2). Triple negative breast cancer, which accounts for 15–20% of all breast cancer cases, and has a highly aggressive characteristic with higher rates of distant recurrence and shorter overall survival compared to other subtypes of breast cancer [1]. Triple negative breast cancer is a heterogeneous breast cancer with various subtypes, and target treatment researches are actively pursued according to each subtype [2]. However, additional research is needed until the treatments developed in such studies are applied to patients. Therefore, therapy to treat TNBCs is largely dependent on chemotherapy using taxane, platinum agents, and anthracycline. However, these treatments have a limited duration response due to the high incidence of resistance and recurrence, as

well as adverse toxic effects. Therefore, many studies are being conducted to identify new target therapies that can be effectively applied in TNBC. As reported in the TCGA database, alteration of RB and CCND1 occurs in 22% of TNBC cases, and mutation of *TP53* accounts for more than 80% of these cases [3]. Thus, dysregulation of the G1 cell cycle checkpoint frequently occurs in TNBC. This aberrant cell cycle regulation results in increased mutation burden because of the high proliferation rate and replication stress accumulation observed at higher Ki-67 levels in TNBCs, resulting in genomic instability [4]. In other words, cell cycle checkpoint defects promote DNA replication and cell division and induce accumulation of damaged DNA, resulting in increased genetic instability. These features have been proposed under the concept of synthetic lethality to inhibit other cell cycle checkpoints that were normally maintained, leading to cell death due to increased genetic instability through abnormal cell cycle progression.

WEE1 is a tyrosine kinase that acts as a cell cycle regulator in the G2/M and S phase through inhibitory phosphorylation of CDK1 and CDK2 [5, 6]. AZD1775, a small molecular inhibitor of WEE1, was shown to cause DNA damage accumulation and apoptosis when applied with DNA damage agents to various *TP53*-mutated cancers cell lines [7, 8]. In addition, AZD1775 has been shown to induce cytotoxic effects on cancer cells independent of *TP53* mutation [9-11] due to the activation of CDK1 by WEE1 inhibition, leading to early mitotic entry and mitotic catastrophe [12]. WEE1 also appears to be involved in replication fork stabilization and replication origin firing [13, 14]. Clinical studies are underway despite the lack of studies investigating the mechanism of action of WEE1 inhibitors in breast cancer. Therefore, preclinical research is urgently needed to investigate the anticancer effects and mechanism of WEE1 inhibitors. Studies of the effects of WEE1 inhibitors on cell cycle regulation and genomic instability are likely to provide valuable information for

development of effective therapy for TNBC, which has high genetic instability and is currently primarily treated using DNA damage chemotherapy.

In the case of HR non-functional cancer, treatment with PARP inhibitor is a promising therapeutic strategy for inducing synthetic lethality. The PARP inhibitors olaparib and talazoparib were approved by the FDA as a single agent for treatment of metastatic breast cancer with the breast cancer type 1/2 susceptibility protein (*BRCA1/2*) germline mutation. Sensitivity to PARP inhibitor is determined based on the homologous recombination defect (HRD), which includes germline and somatic *BRCA1/2* mutation status of the cancer. However, inherited *BRCA1/2* mutations only account for about 5.3% of all breast cancers and less than 15% of TNBCs [3, 15]. Therefore, the application of PARP inhibitors is limited to patients with TNBC subtype with germline *BRCA1/2* mutation or HRD. Recently, combination therapies with various drugs that can inhibit HR capacity have been proposed in order to expand the utility of PARP inhibitors. Indeed, it has been reported that the antitumor effects of

PARP inhibitors are enhanced when HRD phenotype is induced by directly or indirectly regulating DNA repair molecules such as IGF1R, HDAC, ATR and ATM inhibitor [16-19]. WEE1 inhibitor is also reported to cause DNA damage accumulation and increase sensitivity to DNA damaging agents. These results suggest that WEE1 inhibitors may increase the anti-tumor effects of PARP inhibitors through HR regulation in BRCA proficient TNBCs.

This study examined the anti-tumor effect of WEE1 inhibitor, AZD1775, on TNBC cells and found that it induced DNA damage by inducing aberrant cell cycle progression. This DNA damage accumulation caused caspase-3 dependent apoptosis. In addition, AZD1775 has been shown to reduce HR capacity by inhibiting RAD51 foci formation. These results suggest that AZD1775 can sensitize PARP inhibitor by inducing homologous deficiency in TNBC cells. Indeed, in our study, combined treatment with AZD1775 and PARP inhibitor synergistically increased DNA damage accumulation and apoptotic cell death. More importantly, our results provide a

rationale for conducting clinical trials evaluating the effectiveness of using PARP inhibitor combined with AZD1775 to treat TNBC patients.

Material and methods

1. Reagents

AZD1775 and olaparib (AZD2281) were provided by AstraZeneca (Macclesfield, UK). Both reagents were dissolved in dimethyl sulfoxide (DMSO) to prepare 10 mmol/L stock solution.

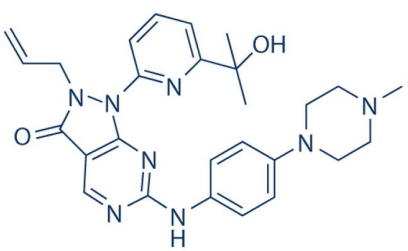

AZD1775 Molecular Weight(MW): 500.6

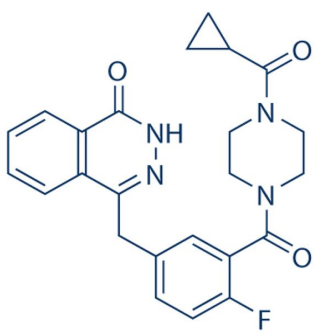

Olaparib Molecular Weight (MW): 434.46

2. Cell lines and cell culture

Human breast cancer cells (MDA-MB-157, MDA-MB-231, MDA-MB-468, HCC1143, HCC1937, BT-549, Hs 578T) were purchased from the American Type

Culture Collection (ATCC, Manassas, VA, USA) and authenticated by short tandem repeat analysis. All cell lines were banked and passaged for less than 6 months before use. During storage, cultures were maintained in a humidified atmosphere of 5% CO_2 and 37℃ in RPMI-1640 (Welgene, Inc., Daegue, South Korea) supplemented with 10% FBS (GIBCO, Thermo Fisher Scientific Inc., Waltham, MA, USA) and 10 μg/mL gentamicin (Cellgro, Manassas, VA, USA).

3. Cell growth inhibition assay

Cells were seeded at a density of 3 to 8×10^3 cells per well in 96-well plates and incubated overnight at 37°C. The cells were then treated with either AZD1775 or olaparib alone or with a combination of AZD1775 and olaparib at specific concentrations for 5 d. Following treatment, MTT solution was added to each well and the plates were incubated for 4 h at 37°C before the medium was removed. After dissolving the resulting formazan crystals with DMSO, cell viability was evaluated by

measuring the absorbance of each well at 540 nm using a VersaMax™ microplate reader (Molecular Devices, Sunnyvale, CA, USA). The combined effects of AZD1775 and olaparib were assessed using the Calcusyn software (Biosoft, Cambridge, UK). The combination index (CI), which is used to evaluate the effects of the two-drug combinations, was calculated using the Chou-Talalay method [20]. Drug synergism was defined by CI values < 0.8, while antagonism was indicated by values >1, and additive effects were indicated by values > 0.8

4. Western blot anlaysis

Cells were collected after drug treatment, washed with ice-cold PBS, and incubated in extraction buffer [50 mM Tris-Cl (pH 7.4), 150 mM NaCl, 1% NP40, 0.1% sodium deoxycholate, 0.1% sodium dodecyl sulfate (SDS), 50 mM sodium fluoride, 1 mM sodium pyrophosphate, 2 mM phenylmethylsulfonyl fluoride, 1 mg/mL pepstatin A, 0.2 mM leupeptin, 10 μg/mL aprotinin, 1 mM sodium vanadate, 1 mM

nitrophenylphosphate, and 5 mM benzamidine] on ice for 30 min. The lysates were cleared by centrifugation at 13,000 rpm for 20 min. Equal amounts of proteins were separated on an 8%–15% SDS-polyacrylamide gel, after which the resolved proteins were transferred onto nitrocellulose membranes and the blots were probed with primary antibodies overnight at 4℃. Antibodies against p53(Do-1), CDK1 p34(17), WEE1, RAD51(H-92), Chk1(FL-476) and Chk2(A-2) were obtained from Santa Cruz Biotechnology (Santa Cruz, CA, USA). Antibodies against caspase 3, p-CDK1 (Tyr15), p-WEE1 (Ser642), MYT1, p-Chk1 (Ser345), p-Chk2 (Thr68) and Mre11 (31H4) were acquired from Cell Signaling Technology (Beverley, MA, USA). Anti-phosphorylated histone H2AX (clone JBW301, Millipore; Billerica, MA, USA) and anti-PARP (BD Biosciences; Bedford, MA, USA) were also purchased, as was α-tubulin antibody (Sigma Aldrich; St. Louis, Missouri, USA) which was used as a control. Antibody binding was detected using an enhanced chemiluminescence system

according to the manufacturer's protocols (Amersham Biosciences; Piscataway, NJ, USA).

5. Cell cycle analysis

Cells treated with AZD1775 and olaparib were harvested, fixed in 70% ethanol, and then stored at -20°C, after which they were dissolved in 10 μg/mL RNase A (Sigma Aldrich; St. Louis, Missouri, USA) at 37°C for 20 minutes. Next, the cells were treated with 20 μg/mL propidium iodide (Sigma Aldrich; St. Louis, Missouri, USA) and the DNA contents of the cells (10,000 cells per experimental group) were measured using a Fluorescence-activated Cell Sorting (FACS) Calibur flow cytometer (BD Biosciences).

6. Edu-BrdU dual pulse labeling

Before cell harvest, cells were treated with 10 mM EdU for 1 h followed by 20 mM BrdU for 15 min. Next, cells were fixed in 70% ethanol and then stored at -20°C. DNA denaturation was performed in 4M HCl for 20 min at room temperature, after which cells were resuspended in phosphate/citric acid buffer. EdU click reaction was then conducted using a Click-iT EdU Flow Cytometry Assay kits (Thermo Fisher Scientific Inc., Waltham, MA, USA). FITC-conjugated anti-BrdU (BD Biosciences; Bedford, MA, USA) used to investigate the BrdU incorporation level. Next, the cells were treated with 7-AAD (BD Biosciences; Bedford, MA, USA) and fluorescence was measured using a Fluorescence-activated Cell Sorting (FACS) Calibur flow cytometer (BD Biosciences; Bedford, MA, USA). Next, pacific blue-conjugated phospho-histone H3(Ser10) and Click-iT EdU Flow Cytometry Assay kits (Thermo Fisher Scientific Inc., Waltham, MA, USA) were used to identify mitotic entry status.

7. Comet assay

An alkaline comet assay was conducted using a Trevigen Comet Assay kit (Trevigen, Gaithersburg, MD, USA) according to the manufacturer's protocols. Tail intensities were measured with the Comet assay IV program (Andor Technology, Belfast, UK).

8. Immunofluorescence assay

Cells were plated on poly-L-lysine coated coverslips. After 48 h, the cells were treated with AZD1775 and/or olaparib. After 2 d, cells were fixed in 3.7% paraformaldehyde and permeabilized with 0.5% Triton X-100 in PBS (PBS-T). Coverslips were then mounted onto slides using Faramount aqueous mounting medium (Dako, Glostrup, Denmark), after which immunofluorescence was visualized using a Zeiss LSM 510 laser scanning microscope.

9. Homologous recombination repair deficiency assay

Cells were transfected with 10 μg of DR-GFP cDNA using lipofectamin. After 24 h, cells with chromosomally integrated constructs were selected by adding 1 mg/mL G-418 (Takara Bio USA; Mountain view, CA, USA) and 0.75 μg/mL puromycin for 2 days. Next, samples were transfected with 5 μg I-Sce1 plasmid using lipofectamine for 2 h, then treated with AZD1775. After 2 d, cells were trypsinized and GFP-content was determined in live cells using flow cytometry.

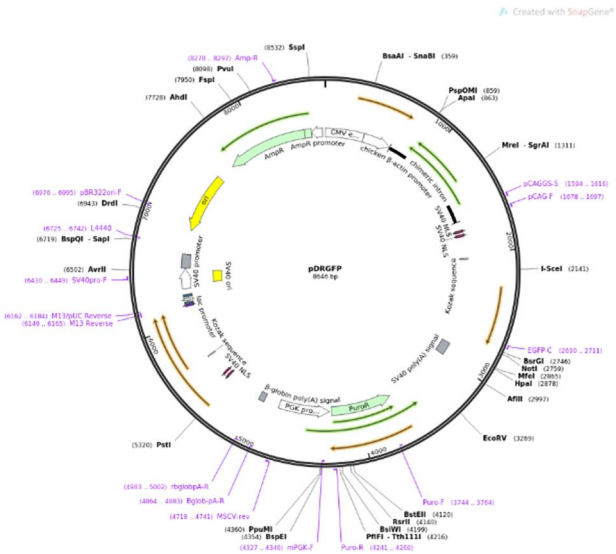

pDR-GFP

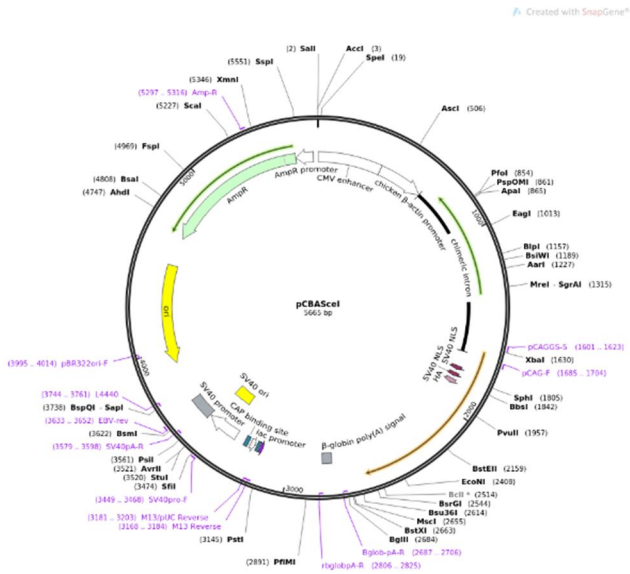

pCBA-SceI

10. In vivo study

All animal experiments were conducted in the animal facility of Seoul National University (Seoul, South Korea) in accordance with institutional guidelines and prior approval from the Institutional Animal Care and Use Committee (IACUC) committee. To measure the *in vivo* activity of AZD1775 and/or olaparib, 21 female Balb/c athymic nude 5-wk-old mice were purchased from Central Lab Animal Inc. (Seoul,

South Korea). MDA-MB-231 cells (1×10^8) were subcutaneously injected into each mouse, after which the size of the resulting tumors and body weight of each mouse were measured. When the tumor volume reached 200 mm^3, the mice were randomly divided into different treatment groups (five per group) and received vehicle, AZD1775, olaparib, or a combination of AZD1775 and olaparib. AZD1775 60 mg/kg and olaparib 40 mg/kg were administered via oral gavages once daily for 28 consecutive days. Tumor volume was calculated using the following formula: ($width^2$ × height)/2. At the end of the measurement period, the mice were sacrificed with CO_2 and the tumors were excised for further analysis.

11. Statistical analysis

Data were analyzed using SigmaPlot version 9.0 (Systat Software Inc., San Jose, CA, USA). All results were expressed as the means ± standard error (SE). A two-sided

Student's *t*-test was used when appropriate. *p*-values <0.05 were considered statistically significant and those <0.1 were considered meaningful.

Results

1. AZD1775 induces apoptotic cell death in TNBC cells.

The percentage of viable cells from eight TNBC cell lines after treatment with the WEE1 inhibitor AZD1775 were measured by MTT assay and IC_{50} (Fig. 1). TNBC cells have a heterogenous response to AZD1775 with IC50 values ranging 0.13 to 0.79 μmol/L. Triple negative breast cancer cells had a heterogenous response to AZD1775, with IC_{50} values ranging 0.19 to 0.82 μmol/L. Based on these values, MDA-MB-231 and BT-549 cells with IC_{50} values lower than 0.5 μmol/L were nominated as sensitive cells. MDA-MB-468 cells were characterized as less sensitive according to the IC_{50} value, which was higher than 0.5 μmol/L. Decreased phosphorylation of CDK1 and CDK2, direct targets of WEE1, confirmed that AZD1775 effectively downregulated target kinase activity (Fig. 2, top). Quantitation of protein

expression resulted in decreased inhibitory phosphorylation of CDK1 when treated with AZD1775 (gray bar) compared to the control (black bar) (Fig. 2, bottom). Previously, the dependence of WEE1 inhibitor sensitivity on p53 dependence was not clear [21]. To investigate whether *TP53* mutation status was associated with WEE1 inhibitor sensitivity, *TP53* mutation status was evaluated using the CCLE database. The sensitivity of AZD1775 was variable even though all TNBC cells failed to function properly because of the *TP53* hotspot mutation. (Fig. 1 & Table 1). In addition, there was no relationship between AZD1775 sensitivity and p53 protein expression levels among TNBC cell lines (Fig. 3). The sub-G1 population indicating to the fragmented DNA expressed by apoptosis was increased in sensitive cells to AZD1775 (Fig. 4). These data demonstrate that the anti-proliferative effect of AZD1775 in TNBC cells was not dependent on the state of p53. The anti-proliferative effect induced by AZD1775 was demonstrated by apoptosis using Annexin V assay

(Fig. 5). After treatment with AZD1775 (350 nM), Annexin V positive cells were increased to 47.8% compared with control cells (15.0%) in sensitive MDA-MB-231 cells (p-value < 0.001); however, changes in Annexin V positive cells in response to AZD1775 in less sensitive MDA-MB-468 cells were not significant (18.4% vs. 24.6%, p-value = 0.08). This apoptosis was demonstrated by an increase in protein levels of cleaved PARP and caspase-3 (Fig. 6).

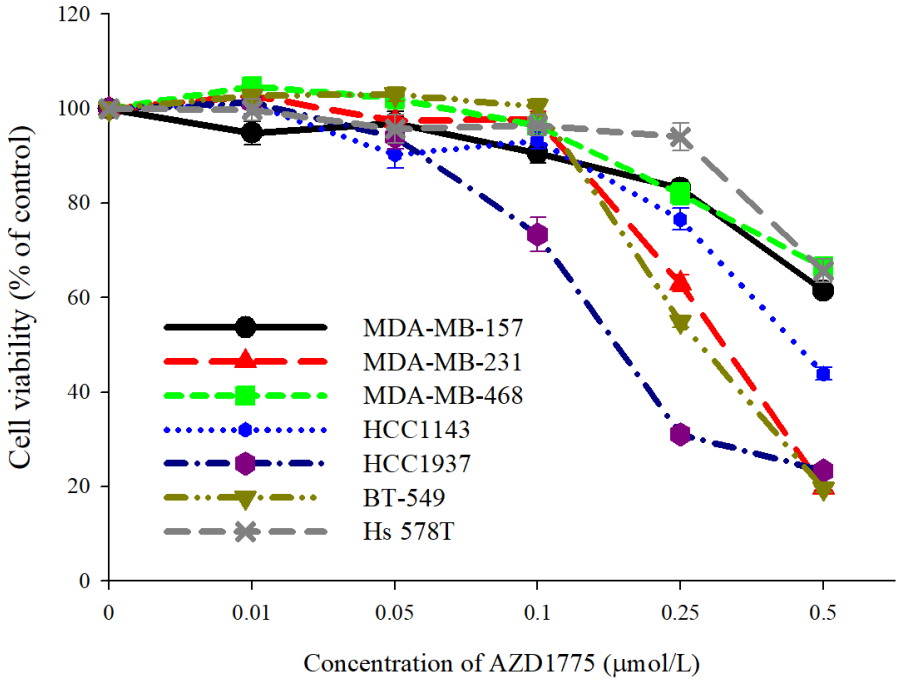

Figure 1. Anti-proliferative effect of AZD1775 Growth inhibition was measured with an MTT assay. Cells were treated with increasing doses of AZD1775 for 5 d. The percentage of surviving cells is presented in a graph with SE bars ($n = 3$).

Table 1. IC_{50} values of AZD1775 in TNBC cells

Cell lines	*TP53* mutation status	*BRCA1/2* mutation status	IC_{50} of AZD1775 (μmol/L)
MDA-MB-157	P88fsX52	wt	0.5529
MDA-MB-231	R280K	wt	0.3550 ± 0.01
MDA-MB-468	R273H	wt	0.8151
HCC1143	R248Q	wt	0.4538 ± 0.07
HCC1937	R306Stop	G1775fs	0.1881 ± 0.01
BT-549	R249S	wt	0.3381 ± 0.01
Hs 578T	V157F	wt	0.7526

The *TP53* and *BRCA1/2* mutations appeared in our TNBC cells and the cells showed various IC_{50} values in response to the AZD1775 treatment, even when the *TP53* mutation was present. The IC_{50} values were calculated using SigmaPlot.

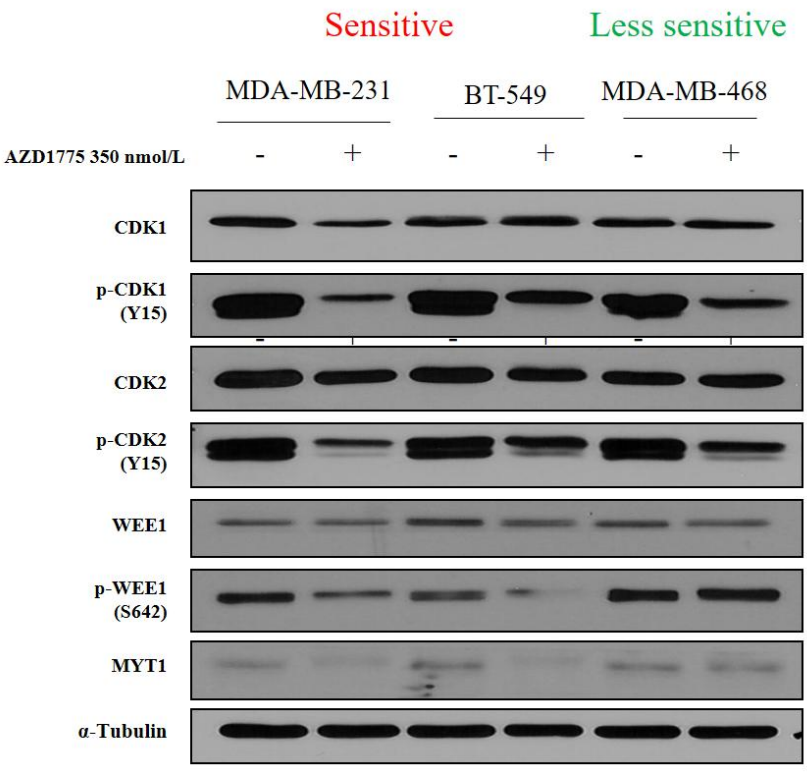
Sensitive
Less sensitive
MDA-MB-231
BT-549
MDA-MB-468
AZD1775 350 nmol/L
- + - + - +
CDK1
p-CDK1 (Y15)
CDK2
p-CDK2 (Y15)
WEE1
p-WEE1 (S642)
MYT1
α-Tubulin

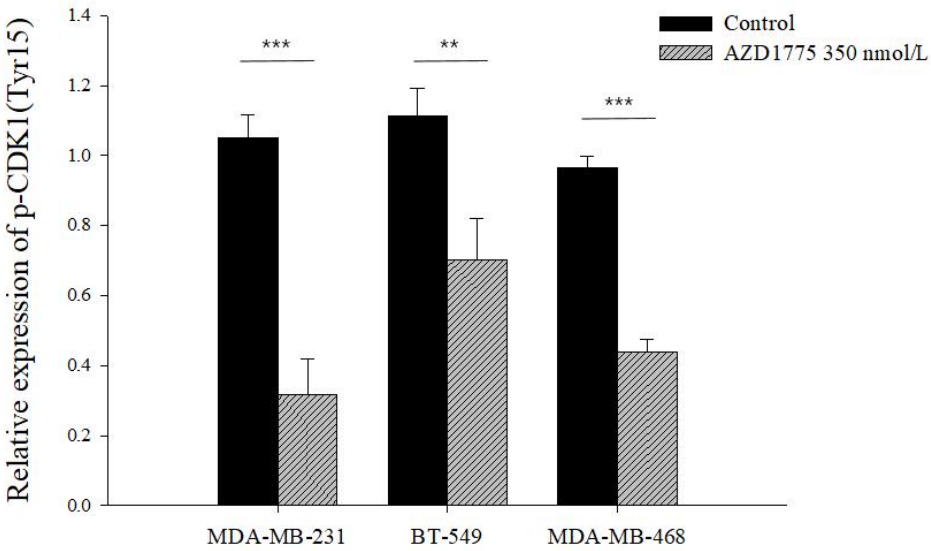
Relative expression of p-CDK1(Tyr15)
1.4
1.2
1.0
0.8
0.6
0.4
0.2
0.0
***
**
***
Control
AZD1775 350 nmol/L
MDA-MB-231
BT-549
MDA-MB-468

Figure 2. Kinase activity of WEE1 was inhibited by AZD1775 After AZD1775 treatment for 5 d, the Tyr15 residue of CDK1 and CDK2 represents the kinase activity of WEE1 and the activation state of WEE1 is shown by phosphorylation of its Ser642 residue. MYT1 is known to play a compensatory role in WEE1. α-Tubulin was used as a loading control and phosphorylation of the Tyr15 residue of CDK1 was normalized using Image J. *Column*; the means of three independent experiments; *Bars*, ±SD. $^{**}P<0.01$; $^{***}P<0.001$.

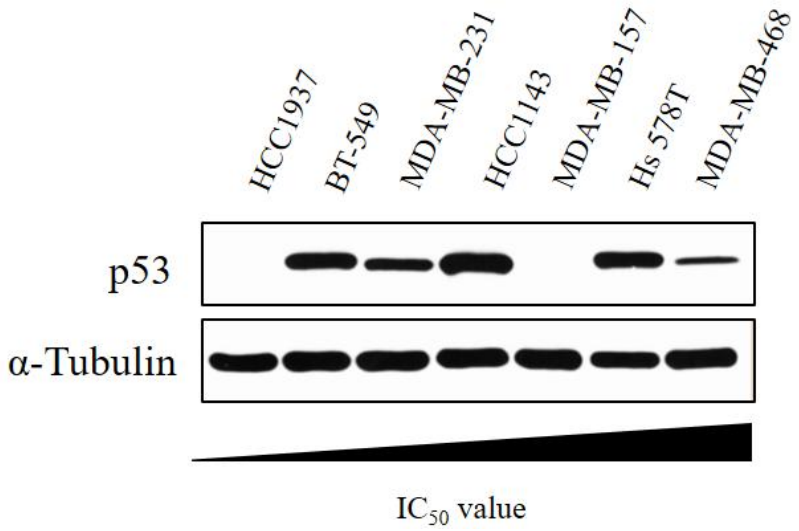

Figure 3. p53 protein expression level of TNBC cells with increasing IC_{50} value

No correlation between p53 expression and AZD1775 sensitivity was observed in TNBC cells.

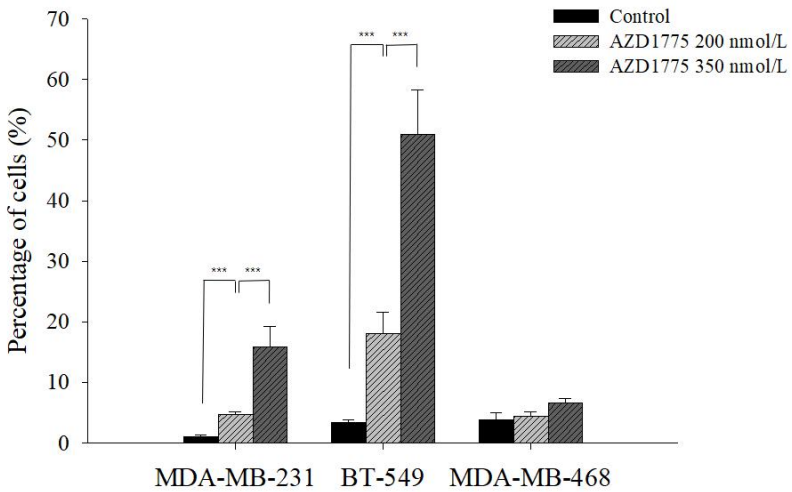

sub-G1 population	Control (%)	200 nmol/L AZD1775 (%)	350 nmol/L AZD1775 (%)
MDA-MB-231	1.1	4.8	15.9
BT-549	3.4	18.1	51.0
MDA-MB-468	3.8	4.5	6.7

Figure 4. The sub-G1 population was increased by AZD1775 treatment TNBC cells were treated with AZD1775 350 nmol/L of 5 d. The DNA content of the TNBC cells was measured by flow cytometry using PI staining. The sub-G1 proportion is shown in the bar graph. The sub-G1 population increased with increasing concentrations of AZD1775 in sensitive cells. Control: black bar, 200 nmol/L AZD175: gray bar, 350 nmol/L AZD1775: dark gray bar. MDA-MB-231; Control: 1.1%, 200 nmol/L AZD1775: 4.8%, 350 nmol/L AZD1775 15.9%, BT-549; Control:

3.4%, 200 nmol/L AZD1775: 18.1%, 350 nmol/L 51.0%. Less sensitive cell MDA-MB-468; Control: 3.8%, 200 nmol/L AZD1775: 4.5%, 350 nmol/L AZD1775: 6.7%. ***P<0.001.

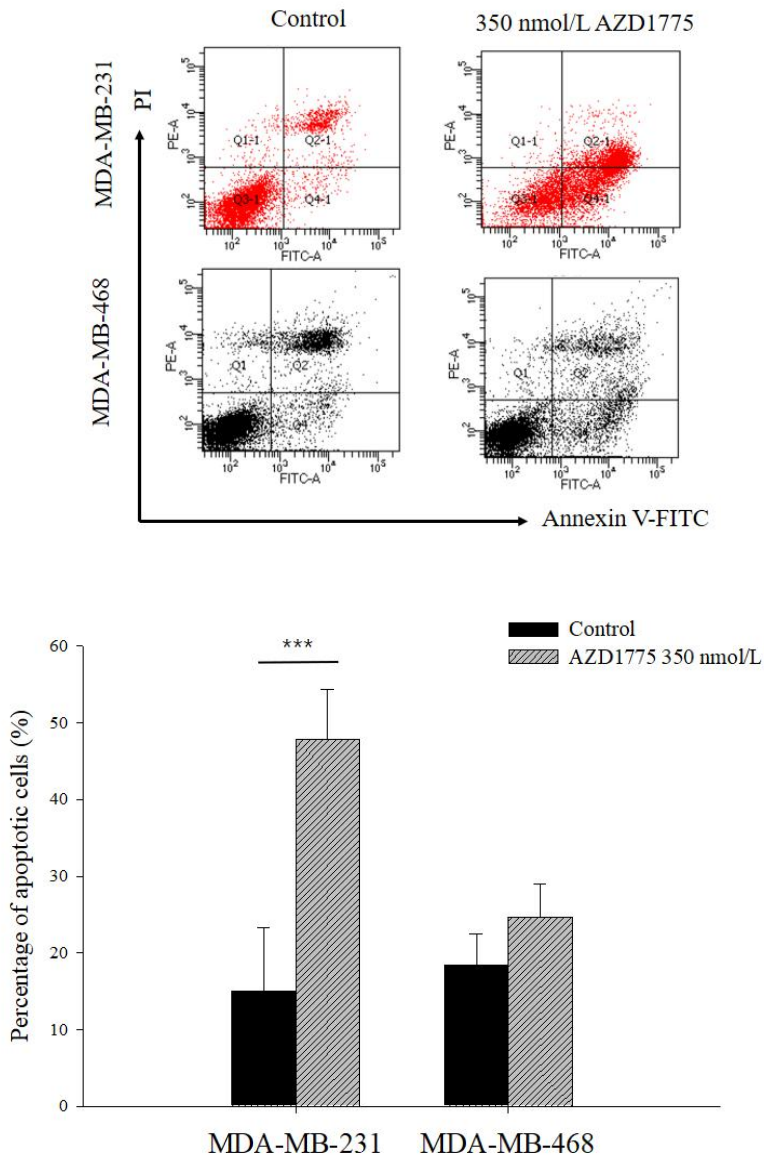

Figure 5. AZD1775 induces apoptotic cells in sensitive TNBC cells TNBC cells were treated with AZD1775 at 350 nmol/L for 5 d. Annexin-V PI staining was performed to identify apoptotic cells. ***P<0.001.

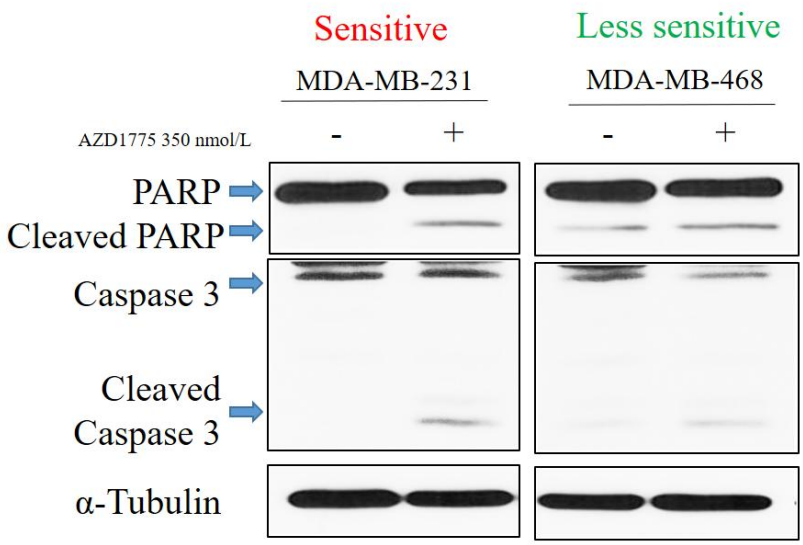

Figure 6. Caspase dependent apoptosis induced by AZD1775 After 5 d of treatment with AZD1775 350 nmol/L, MDA-MB-231 and MDA-MB-468 cells were analyzed by Western blotting and probed with anti-PARP, caspase-3 and α-tubulin antibody. Protein expression of cleaved PARP and caspase 3 was increased in MDA-MB-231 cells, AZD1775 sensitive cell line

2. AZD1775 induces aberrant cell cycle.

WEE1 is widely known as a kinase involved in the G2/M cell cycle checkpoint. Therefore, the cell cycle distribution was confirmed by FACS analysis to investigate the effects of inhibiting WEE1. The populations of cells in S phase increased in sensitive cell lines following AZD1775 treatment in a dose dependent manner (Fig. 7), and these cell cycle changes were also observed at early time points (Fig. 8). To determine how the cell cycle progressed in the S phase by the AZD1775, two different thymidine analogs (BrdU, EdU) were sequentially incorporated to investigate progression of the S phase (Fig. 9). The number of EdU/BrdU (-/+) cells indicating the early S phase and EdU/BrdU (+/+) cells indicating the mid/late S phase increased, confirming that the initiation and progression of S phase was accelerated by AZD1775. Moreover, AZD1775 increased the number of cells expressing mitosis marker p-HH3 in EdU positive cells, indicating the S phase (Fig. 10).

Another notable point is that the long-term exposure of AZD1775 significantly increased the DNA content over 4n (Fig. 11). These results indicate that the mitotic exits were abnormal because of WEE1 inhibition, resulting in an increase in multinucleated cells (Fig. 12), one of the features of mitotic catastrophe [22]. These results suggest that is involved not only in replication initiation but also in mitotic entry and exit and that it exerts influence throughout the cell cycle.

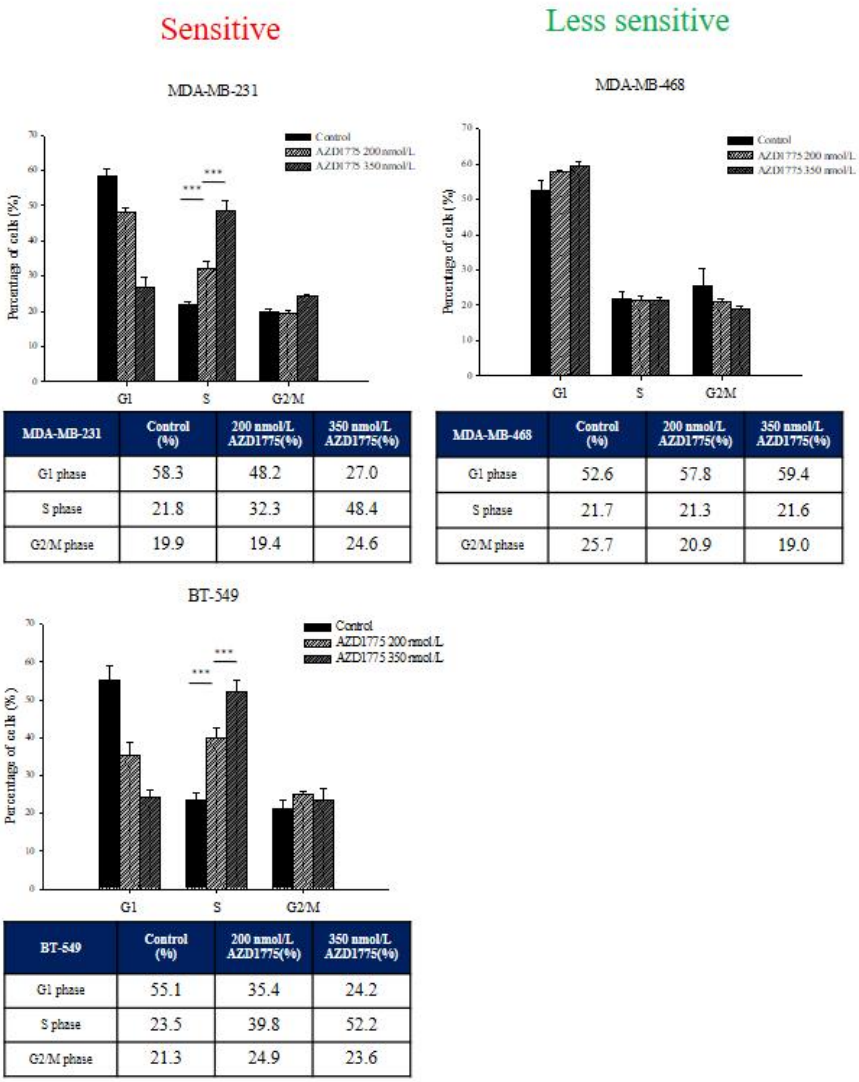

MDA-MB-231	Control (%)	200 nmol/L AZD1775(%)	350 nmol/L AZD1775(%)
G1 phase	58.3	48.2	27.0
S phase	21.8	32.3	48.4
G2/M phase	19.9	19.4	24.6

MDA-MB-468	Control (%)	200 nmol/L AZD1775(%)	350 nmol/L AZD1775(%)
G1 phase	52.6	57.8	59.4
S phase	21.7	21.3	21.6
G2/M phase	25.7	20.9	19.0

BT-549	Control (%)	200 nmol/L AZD1775(%)	350 nmol/L AZD1775(%)
G1 phase	55.1	35.4	24.2
S phase	23.5	39.8	52.2
G2/M phase	21.3	24.9	23.6

Figure 7. S phase accumulation appears in MDA-MB-231 and BT-549 cell lines by AZD1775 TNBC cells were treated with AZD1775 350 nmol/L for 5 d, after which the DNA contents of the TNBC cells were measured by flow cytometry using PI staining. The proportion of cells in each stage of the cell cycle is shown in the bar

graph. In MDA-MB-231 and BT-549 cells, S phase accumulation increased with AZD1775 concentration. The S phase population of MDA-MB-231 cell was 21.8% in the control, but increased to 32.3% in response to 200 nmol/L AZD1775 and 48.4% in response to 350 nmol/L AZD1775. For BT-549, 23.5% of cells were in the S phase in the control, while 39.8% of cells in the AZD1775 200 nmol/L treatment and 52.5% in the 350 nmol/L AZD1775 treatment were in the S phase. In contrast, the S phase population of MDA-MB-468 cells did not change (Control vs 200 nmol/L AZD1775 vs. 350 nmol/L AZD1775, 21.7% vs. 21.3% vs. 21.6%). $^{**}P<0.01$, $^{***}P<0.001$.

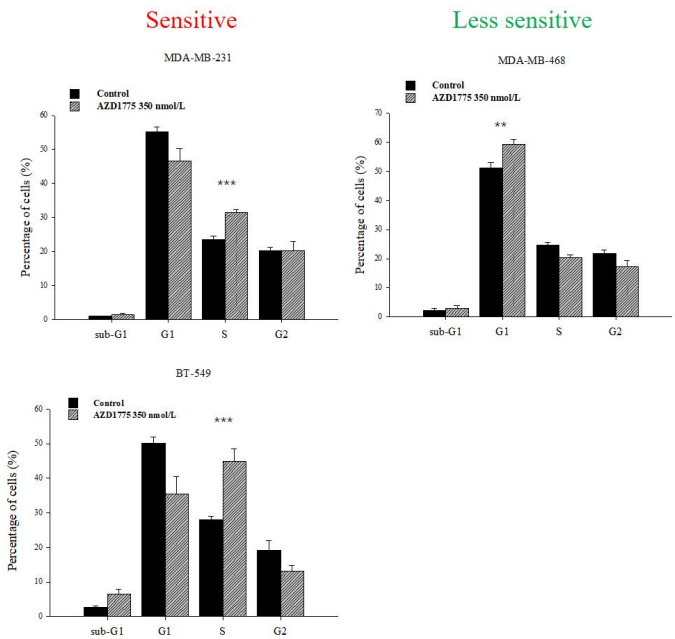

Figure 8. Cell cycle distribution following AZD1775 treatment at an early time point After the indicated dose of AZD1775 was applied for 24 h, the proportion of cells in different phases of the cell cycle was confirmed by flow cytometry. The proportion of MDA-MB-231 cells in the S phase increased to 44.8% in response to AZD1775 (control = 28%), while that of BT-549 increased to 31.6 (control = 23.6%). However, the proportion of MDA-MB-468 cells in the S phase showed no significant change in response to treatment (control vs AZD1775, 24.6% vs 20.3%). $^{**}P<0.01$. $^{***}P<0.001$.

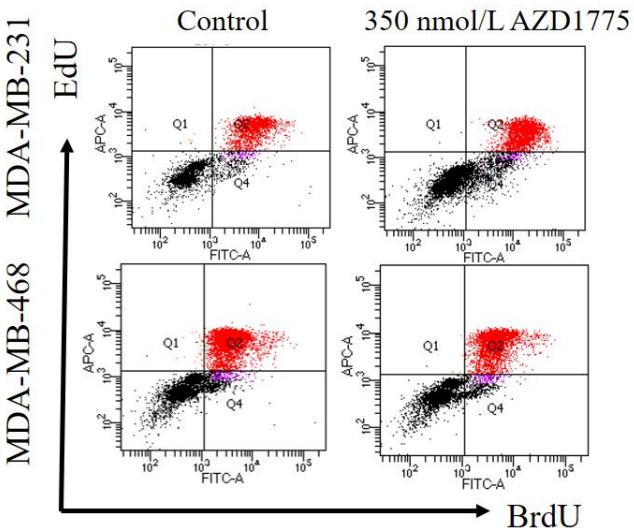

MDA-MB-231	Control	AZD1775 350 nmol/L
Early S (BrdU+/EdU-)	8 %	16.8%
Mid/Late S (BrdU+/EdU+)	34.2%	26.4 %

MDA-MB-468	Control	AZD1775 350 nmol/L
Early S (BrdU+/EdU-)	6.5 %	5.5 %
Mid/Late S (BrdU+/EdU+)	36.5 %	32.2 %

Figure 9. AZD1775 accelerates S phase progression in sensitive cell lines

Following treatment with 350 nmol/L AZD1775 for 24 h, S phase progression was examined by EdU-BrdU dual pulse labeling. EdU/BrdU(-/+) indicates the early S phase, EdU/BrdU(+/+) indicates the post S phase.

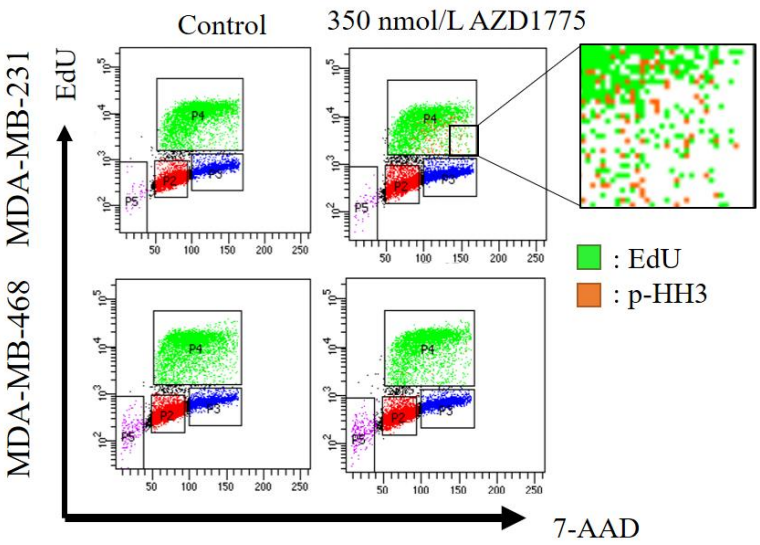

MDA-MB-231	Control	AZD1775 350 nmol/L
Mitotic cells (Edu-/pHH3+)	0.9 %	6.4 %
Early mitotic entry cells (EdU+/pHH3+)	0 %	1.5 %

MDA-MB-468	Control	AZD1775 350 nmol/L
Mitotic cells (Edu-/pHH3+)	1.2 %	3.2 %
Early mitotic entry cells (EdU+/pHH3+)	0 %	0.1 %

Figure 10. Early mitotic entry induced by WEE1 inhibition in the MDA-MB-231 cell line After treatment under the above conditions, p-HH3 (orange color) antibody was applied to TNBC cells that had incorporated EdU (green color) to investigate the S phase and the mitotic phase.

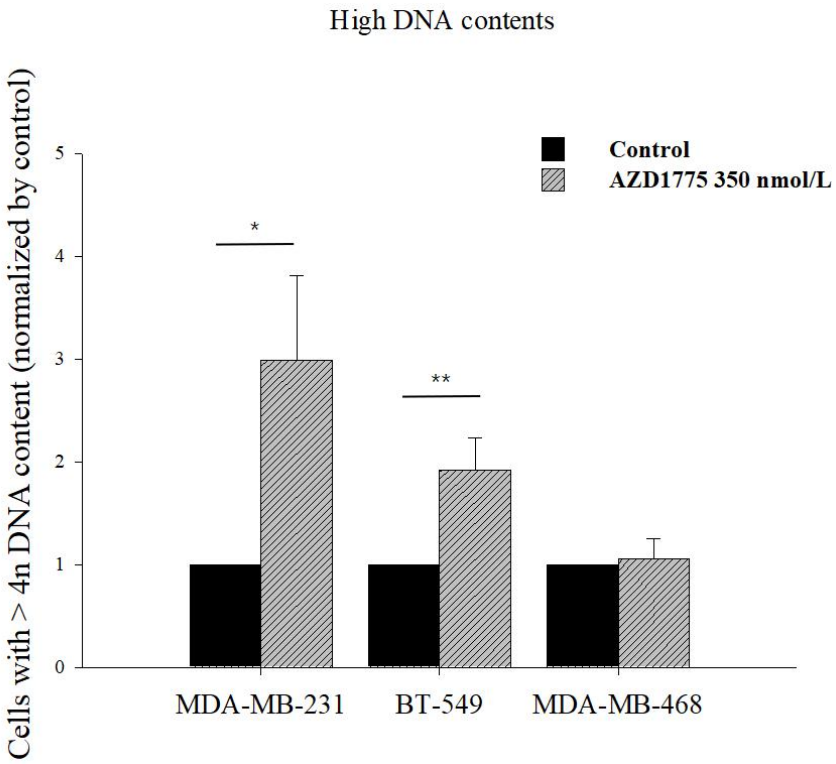

Figure 11. AZD1775 induces an increase in cells with DNA content of more than 4n The TNBC cells were treated with 350 nmol/L AZD1775 for 5 d, after which PI stained cells with high DNA contents were identified by flow cytometry. In AZD1775 sensitive cells, AZD1775 treatment increased the DNA content relative to the control (MDA-MB-231; 3.42 fold, BT-549: 2.03 fold, MDA-MB-468; 1.04 fold). *P<0.05. **P<0.01

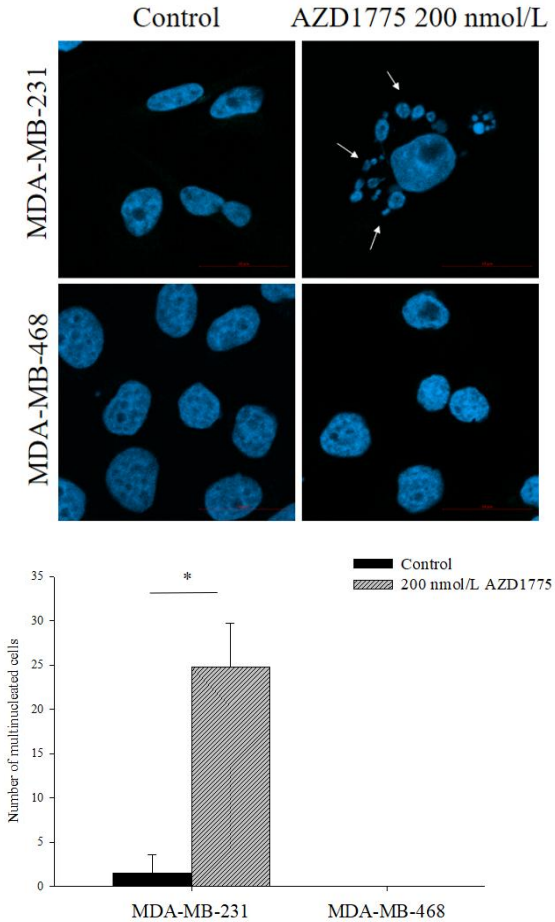

Figure 12. Multinucleated cells increased in MDA-MB-231 cells in response to AZD1775 The nuclei of MDA-MB-231 and MDA-MB-468 cells were stained with DAPI, and multinucleated cells were analyzed by confocal microscopy. Each cell lines count 100 cells and white arrows indicate multinucleated nuclei. The scale bar indicates 20μm, **P*<0.05

3. AZD1775 decreases DSB repair capacity.

Replication stress is one of the causes of DNA damage. Because TNBC has increased replicative stress and a high genomic instability, the aberrant cell cycle induced by WEE1 inhibition will further increase this replication stress and consequently increase the accumulation of damaged DNA. AZD1775 induced replicative stress resulting in Chk1 activation and increased γ-H2AX levels was observed in TNBC cells, regardless of response to AZD1775. However, protein expression levels in the components of the MRN complex were decreased in some TNBC cells. (Fig. 13). We conducted a comet assay to test whether the DNA damage was increased by WEE1 inhibition. The tail length indicating DNA damage was significantly increased in MDA-MB-231 and BT-549 cells following AZD1775 treatment (Fig. 14). These results suggested that AZD1775 would impair DNA damage repair capacity via depletion of HR components. Consistently, depletion of DDR capacity was

confirmed by IFA assay. The increased levels of DNA damage in response to AZD1775 were confirmed by the increase of γ-H2AX foci, but the formation of RAD51 foci, which is involved in DNA strand exchange in HR, was inhibited (Fig. 15). These results suggest that the WEE1 inhibitor reduces HR efficacy.

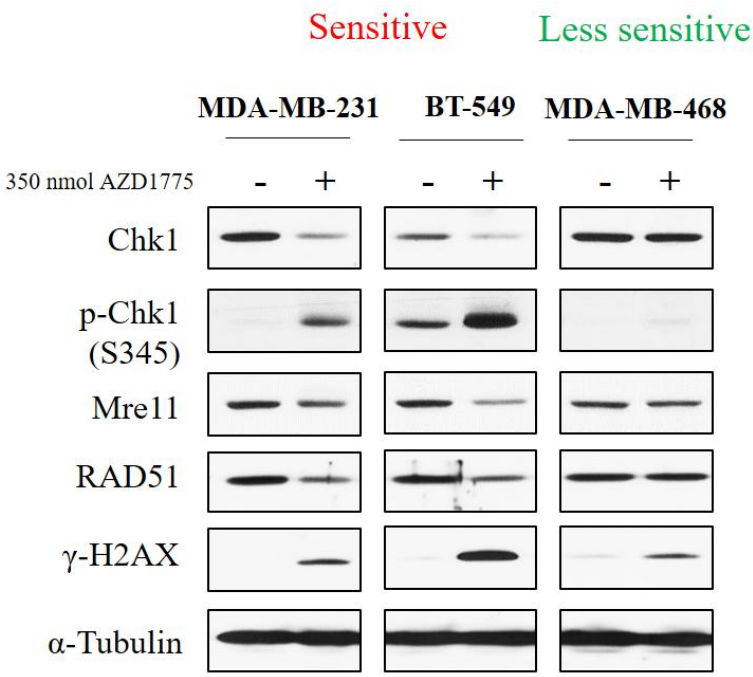

Figure 13. Protein expression of RAD51 and Mre11 decreased in some TNBC cells in response to AZD1775 treatment The expression levels of DNA damage response proteins in TNBC cells were measured by western blotting after 350 nmol/L AZD1775 treatment for 48 h.

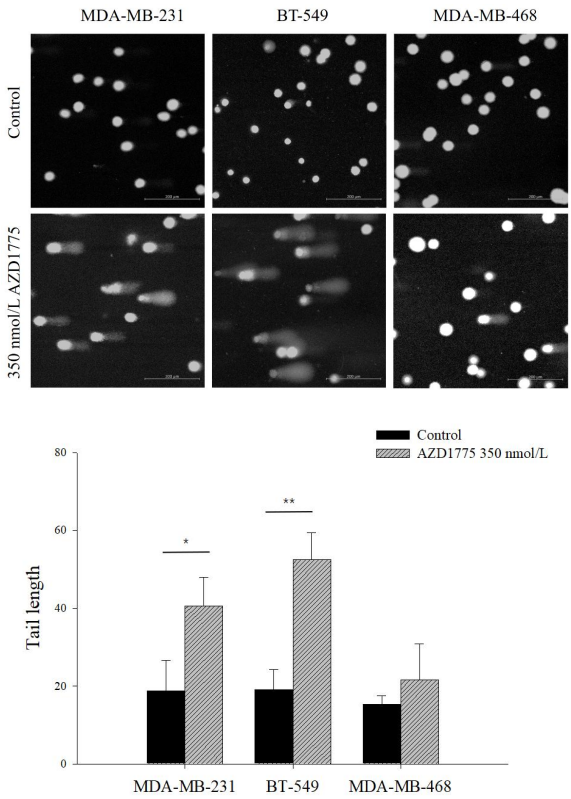

Figure 14. Treatment with AZD1775 causes DNA damage accumulation Cells were treated with 350 nmol/L AZD1775 for 5 d, after which the DNA double strand breaks in each cell were measured by comet assay. Tail length is represented in the bar graph with error bars (±SD). Treatment with AZD1775 resulted in significantly increased tail length in MDA-MB-231 cells but not in MDA-MB-468. The scale bar indicates 200 μm *P<0.05. **P<0.01

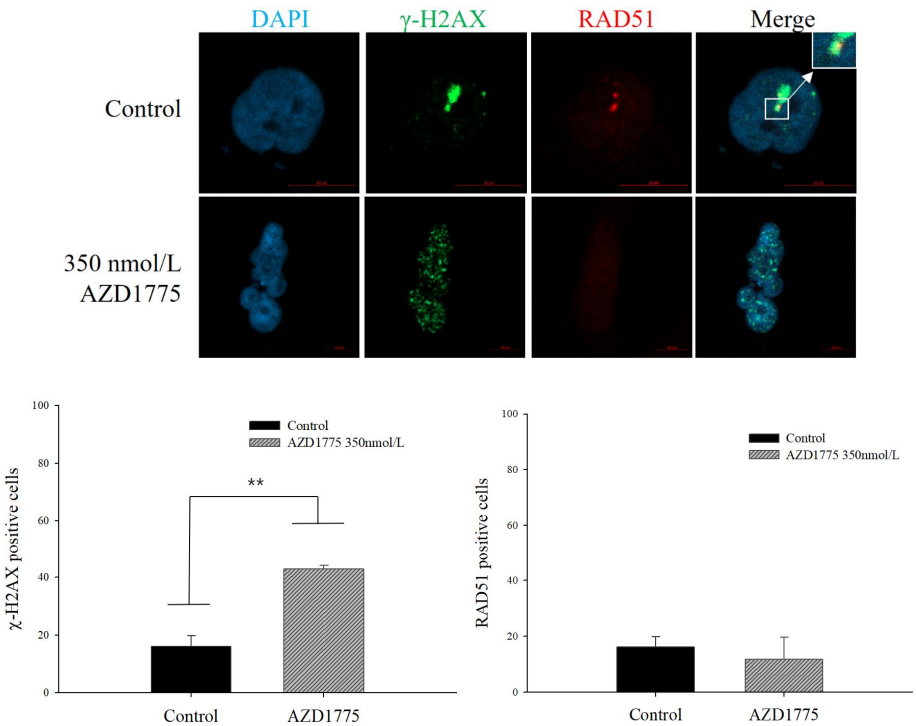

Figure 15. AZD1775 inhibits the formation of RAD51 foci on sites of DNA damage After treatment with AZD1775 at 350 nmol/L for 48 h, RAD51 (Red) and γ-H2AX (Green) foci formation were measured by immunoblotting and confocal microscopy. A total of 100 cells per group were analyzed, and cells with at least 5 foci were regarded as positive. The DNA was counterstained with DAPI (blue). The scale bar indicates 10 μm. ***P*<0.01.

4. Co-administration of olaparib and AZD1775 has a synergistic anti-proliferative effect in TNBC cells.

PARP inhibitor is a target drug that can induce synthetic lethality in the presence of HR defects such as *BRCA1* or *BRCA2* germline mutation. We hypothesized that WEE1 inhibitor could increase the sensitivity of PARP inhibitors by mimicking BRCAness phenotype in TNBC cells. The combination index was calculated to determine if combined treatment with olaparib and AZD1775 had a synergistic effect. This analysis revealed that the anti-proliferative effect of co-administration was at different levels in TNBC cells (Table. 2). Among the seven cell lines, five cells (MDA-MB-157, MDA-MB-231, MDA-MB-468, HCC1937, BT-549) showed synergistic effects, whereas two cells (HCC1143, Hs 578T) showed additive combination effects. MDA-MB-231 cells showing effects of synergistic anti-proliferative effect at low and high dose of AZD1775, and Hs 578T cells did not show such an

effect (Fig. 16). The combination of WEE1 inhibitor and PARP inhibitor showed increased cell death by the sub-G1 population (Fig. 17). Also, AZD1775 increased the sensitivity of the PARP inhibitor more than 6-fold in MDA-MB-231 cells (Fig. 18). Consistent with FACS analysis, combination treatment increased caspase-3 cleavage (Fig. 19). To determine if increased DNA damage induced by olaparib was a result of HR depletion through WEE1 inhibition, the degree of DNA damage was evaluated with AZD1775 and/or olaparib treatment. Dual inhibition further increased DNA damage accumulation compared to mono-treatment (Fig. 20). In addition, the combination treatment of AZD1775 and olaparib increased replication stress, but RAD51 expression, which are involved in repairing DNA damage, were reduced by combination treatment in MDA-MB-231 cells (Fig. 21). To determine if AZD1775 actually affected HR capacity, we conducted an HRD assay. pDR-GFP and endonuclease I-Sce1 were sequentially transfected, after

which the GFP positive cells were counted. In MDA-MB-231 and BT-549 cells, GFP positive cells were decreased by WEE1 inhibition (Fig. 22). These results demonstrate that the WEE1 inhibitor not only induces DNA damage because of aberrant cell cycle progression, but it also reduces the ability of HR. This DNA damage accumulation was found to be induced through reduction of the foci formation of RAD51 with the increase of foci formation of γ-H2AX (Fig. 23), suggesting that WEE1 inhibitor can induce HRD-like phenotype and thus enhance the anti-tumor effect of olaparib. The suppression of HR by WEE1 inhibition would enhance the effects of DNA damage inducing agents, such as cisplatin and ATR inhibitor. To determine if WEE1 inhibitor was effective when administered in combination with other DNA damage inducing agents, a combination index was calculated (Table 3). The results revealed that AZD1775 sensitized TNBC cells to DNA damaging agents by compromising HR capacity

Table 2. Combination index of AZD1775 with olaparib combination treatment

Cell lines	AZD1775 IC_{50} (μmol/L)	olaparib IC_{50} (μmol/L)	1:20 combination IC_{50} (μmol/L)	Combination index (CI value at ED_{50})
MDA-MB-157	0.5529	>10	0.3986	<0.8
MDA-MB-231	0.3550	>10	0.1963	<0.8
MDA-MB-468	0.7651	4.3013	0.0665	<0.8
HCC1143	0.4538	>10	0.4134	>0.8
HCC1937	0.1880	1.5984	0.0605	<0.8
BT-549	0.3381	>10	0.2587	<0.8
Hs 578T	0.7884	>10	0.6053	>0.8

The concentration of AZD1775 was gradually increased from 0.1 to 1μmol/L for 5 d and the AZD1775/olaparib dose ratio was 1:20. Cell growth inhibition was investigated by MTT assay and the combination index was measured using the Calcusyn software.

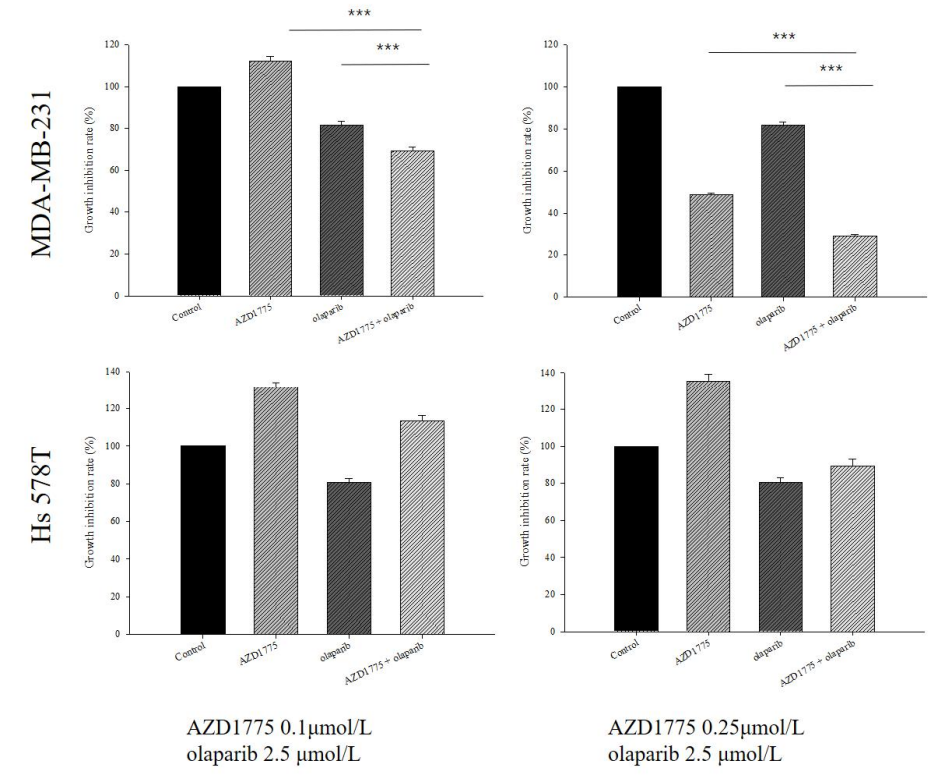

Figure 16. Anti-proliferative effect of combination treatment 0.1 μmol/L and 0.25 μmol/L of AZD1775 were treated with 2.5 μmol/L olaparib for 5d. MDA-MB-231 cells show a synergistic effect with olaparib at low or high dose of AZD1775. Cell growth inhibition was investigated by MTT assay**.** ***P<0.001

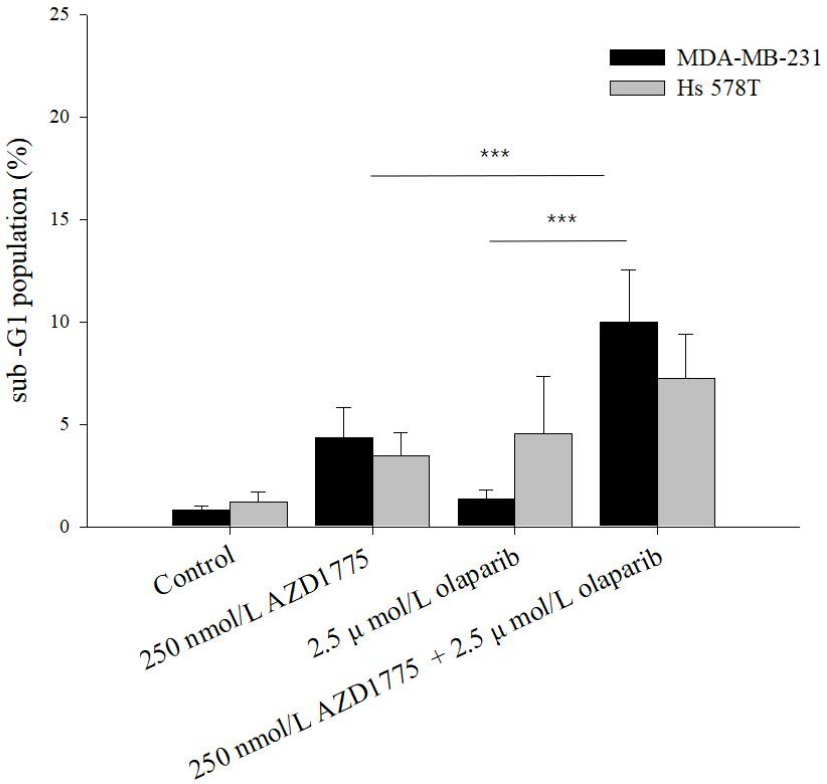

Figure 17. sub-G1 population after combination treatment After treatment with AD1775 350 nmol/L and/or olaparib 2.5 μmol/L for 5 d, sub-G1 population was investigated by flow cytometry. In MDA-MB-231 cells, combination treatment synergistically increased the population of sub-G1 compared to AZD1775 and olaparib alone. ***P<0.001

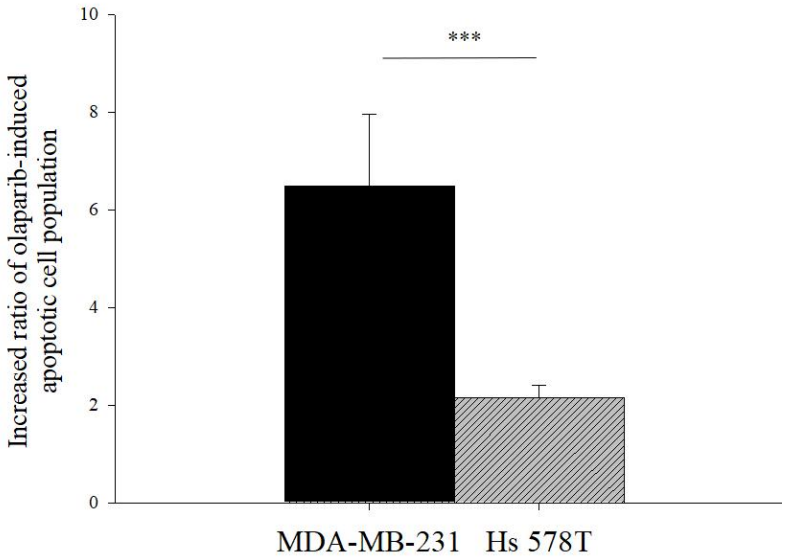

Figure 18. Increased olaparib sensitivity by AZD1775 Combination treatment of AZD1775 increased the sub-G1 population compared to olaparib alone treatment. The sub-G1 population of MDA-MB-231 cells was increased 6.5-fold by combination treatment while Hs 578T cells were doubled. ***P<0.001

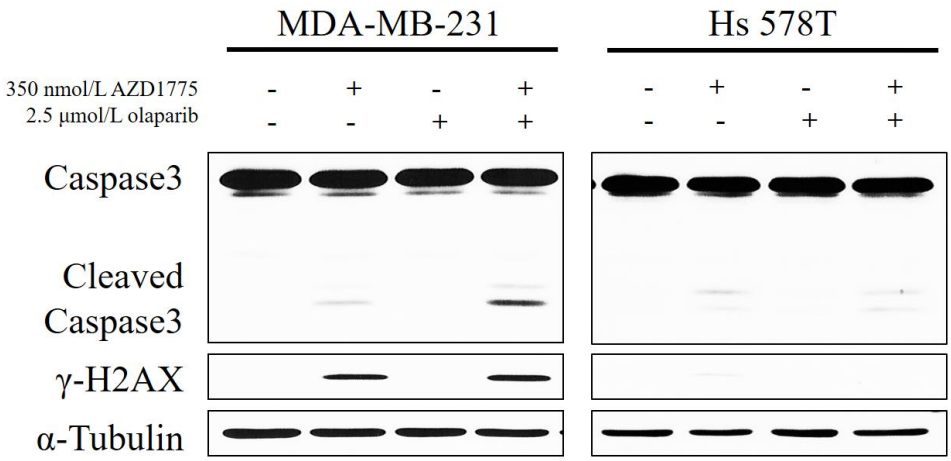

Figure 19. Combined treatment with AZD1775 and olaparib increased cleaved caspase-3 The levels of cleaved caspase-3 were used to confirm cell death caused by apoptosis. The indicated doses of drugs were applied for 5 d.

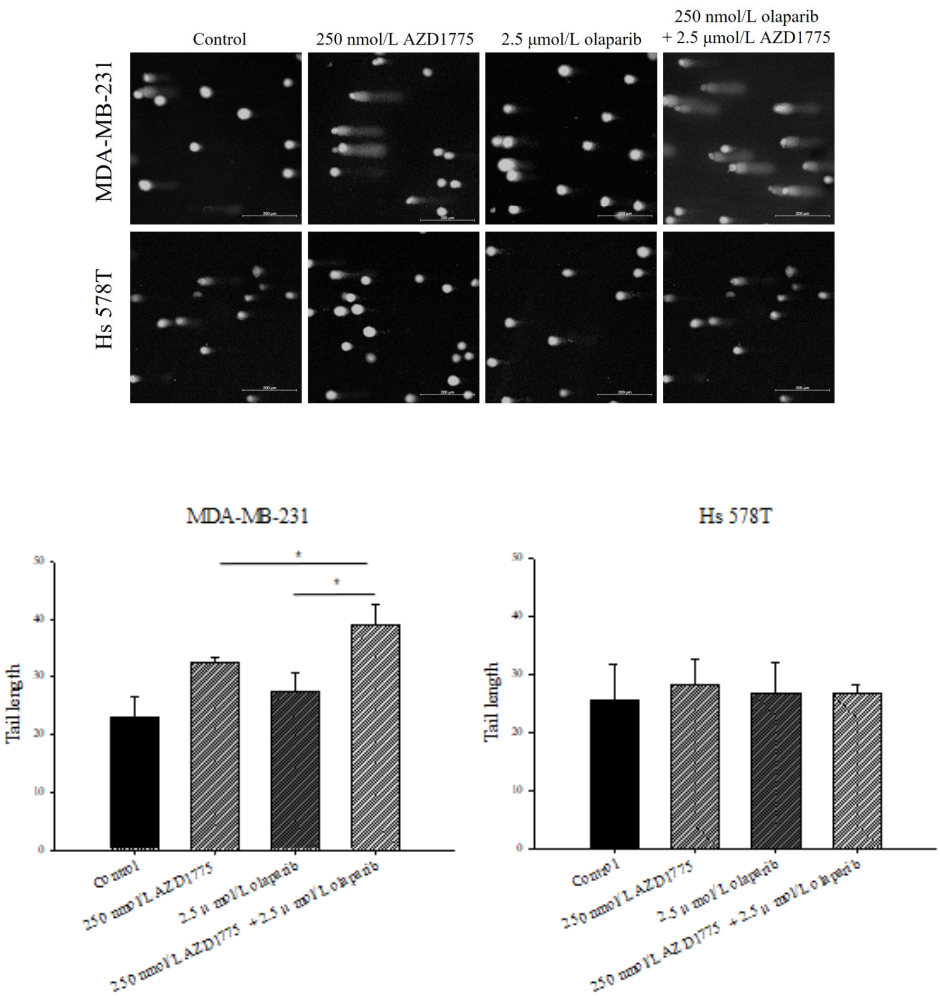

Figure 20. Combination treatment with AZD1775 and olaparib increased DNA damage accumulation compared with single agent treatment Comet assay showed that DNA damage caused by olaparib was further increased by co-treatment with AZD1775. In sensitive cells, DNA damage was significantly increased in combination treatments. The scale bars indicate 200 μm. *P<0.05

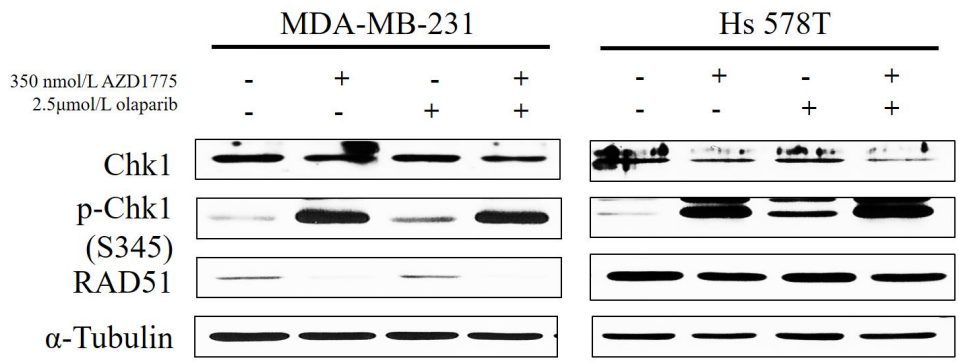

Figure 21. Combination treatment with AZD1775 and olaparib downregulated the protein expression level of DNA damage response molecules After treatment with AD1775 at 350 nmol/L and/or olaparib at 2.5 μmol/L for 48h. p-Chk1(Ser345) indicates whether replication stress occurred, and the protein expression level of RAD51 indicates that the DNA repair capacity is decreased by WEE1 inhibitor. In combination treatments, the ability of DNA repair was decreased like AZD1775 alone treatment.

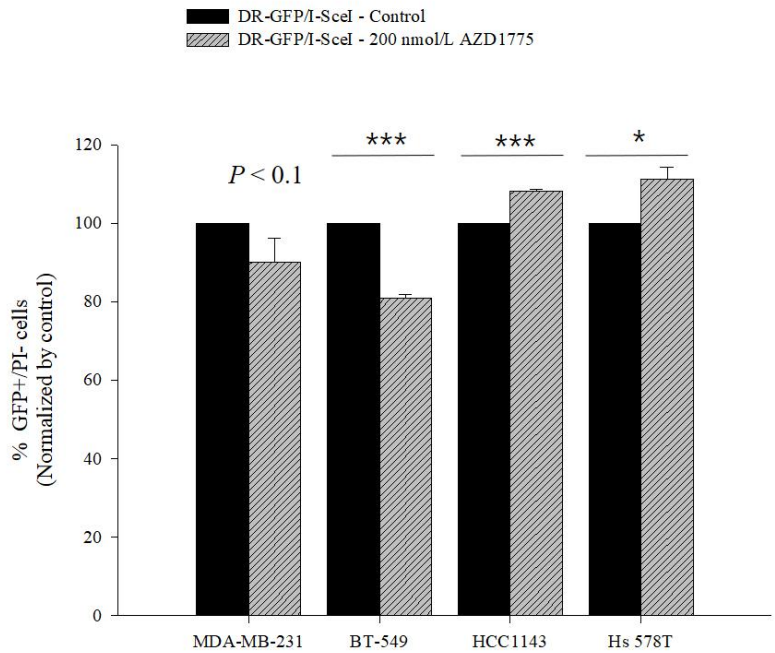

Figure 22. Homologous recombination repair capacity was reduced by AZD1775 treatment GFP positive cells were counted in PI negative cells. Normalization is based on the control values of the counted cell. *P<0.05, ***P<0.001.

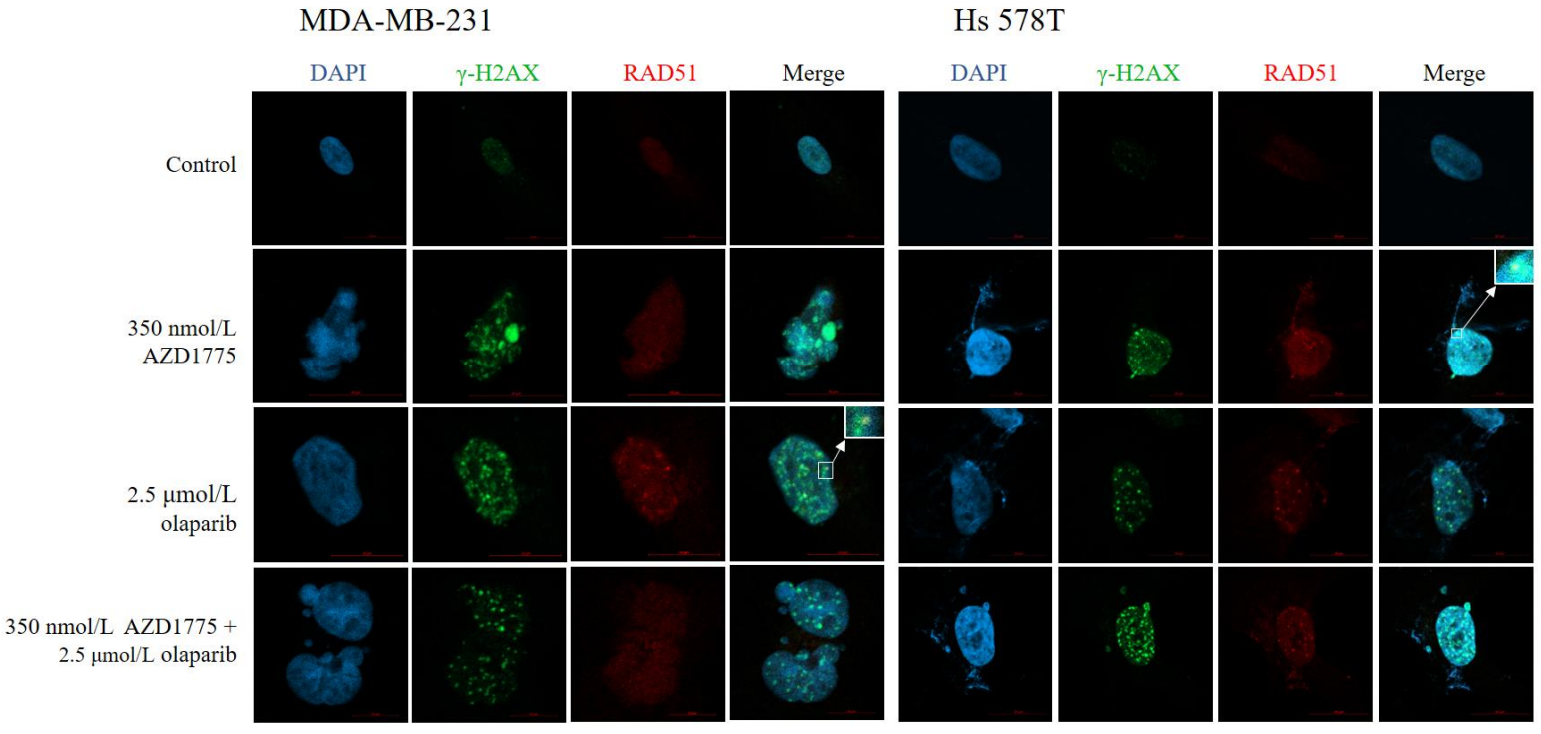
MDA-MB-231
Hs 578T
DAPI
γ-H2AX
RAD51
Merge
DAPI
γ-H2AX
RAD51
Merge
Control
350 nmol/L AZD1775
2.5 µmol/L olaparib
350 nmol/L AZD1775 + 2.5 µmol/L olaparib

Figure 23. AZD1775 inhibits the formation of RAD51 foci caused by olaparib

Decreased HR capacity by WEE1 inhibition was confirmed by formation of RAD51 foci. Blue indicates DAPI, representing DNA, green indicates γ-H2AX, representing the degree of DNA damage, and RAD51 used to confirm HR capacity is indicated by red. RAD51 foci at the DNA damage site caused by olaparib decreased in response to AZD1775 treatment. The scale bar indicates 10 μm.

Table 3. Combined treatment of AZD1775 with cisplatin or ATR inhibitor shows a synergistic anti-tumor effect in TNBC cells

Cell lines	*TP53* mutation status	Combination index(ED_{50}) of Cisplatin	Combination index(ED_{50}) of ATR inhibitor
MDA-MB-157	P88fsX52	0.34	0.3
MDA-MB-231	R280K	0.73	0.2
MDA-MB-468	R273H	0.16	1.1
BT-549	R249S	0.79	1.0
Hs 578T	V157F	0.62	>1

The concentration of AZD1775 was gradually increased from 0.1 to 1μmol/L for 5 d. The AZD1775/cisplatin and AZD1775/ATR inhibitor dose ratio was 1:10. Cell growth inhibition was investigated by MTT assay and the combination index was measured using the Calcusyn software.

5. Combined treatment with AZD1775 and olaparib significantly inhibits tumor growth in a xenograft model of MDA-MB-231 human breast cancer.

To determine whether treatment with AZD1775 and olaparib exerted an anti-tumor effect in vivo in a mouse model, MDA-MB-231 was xenografted into Balb/c nude mice. Treatment with AZD1775 alone delayed tumor growth when compared to the control and showed a significant anti-tumor effect in response to combination treatment (Fig. 24). Moreover, mouse weight was maintained at a constant level regardless of drug treatment, indicating that the drug was tolerated (Fig. 25). In tumor tissues combined with AZD1775 and olaparib, the level of ki-67 was lower than vehicle control and mono-treatment, which means that the ability of proliferation was reduced and it was related to increased apoptosis by TUNNEL assay. The kinase activity of WEE1 decreased by treatment with AZD1775 through the level of p-CDK1(Y15) (Fig. 26). AZD1775 also significantly inhibited tumor growth though

cisplatin combined treatment (Fig. 27). These findings indicate that treatment of AZD1775 with olaparib can be presented as a potential treatment for TNBCs.

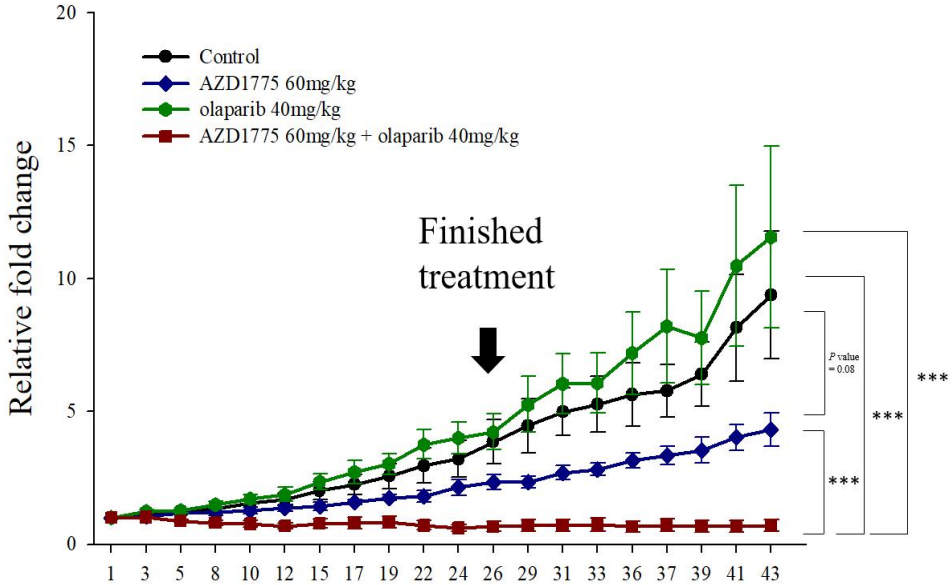

Figure 24. Treatment of AZD1775 with olaprib significantly inhibits tumor growth in a xenograft mouse model of MDA-MB-231 human breast cancer

Balb/c nude mice were injected with 1 x 10^7 MDA-MB-231 cells. Mice were treated with vehicle alone (n=4), 60 mg/kg AZD1775 (n=4), 40 mg/kg olaparib (n=4) and both drugs (n=5). The tumor volumes of each mouse were measured three times a week and are presented as a graph with SE bars. ***P<0.001.

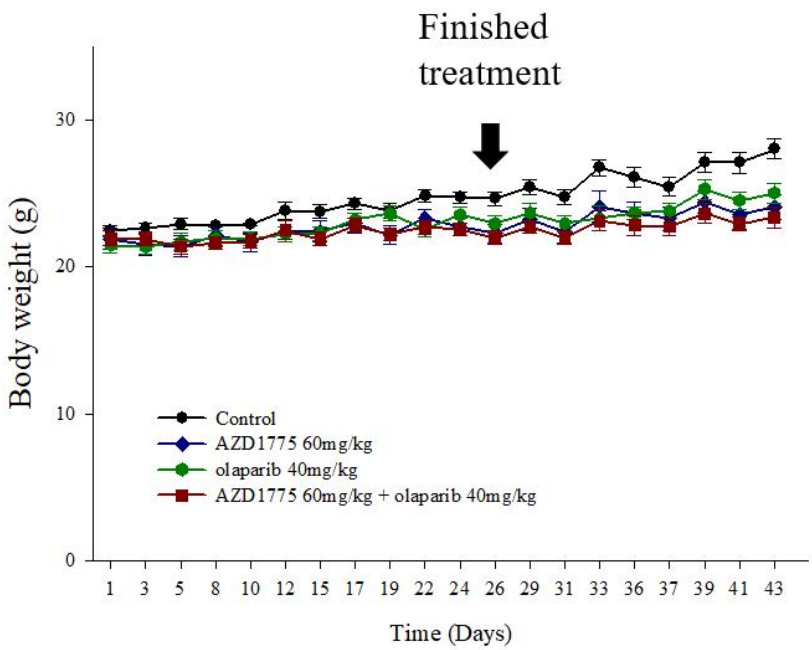

Figure 25. Changes in mouse weight during drug treatment The body weight of each mouse was measured three times a week. No significant difference in weight change was observed between groups. Bars, ±SE.

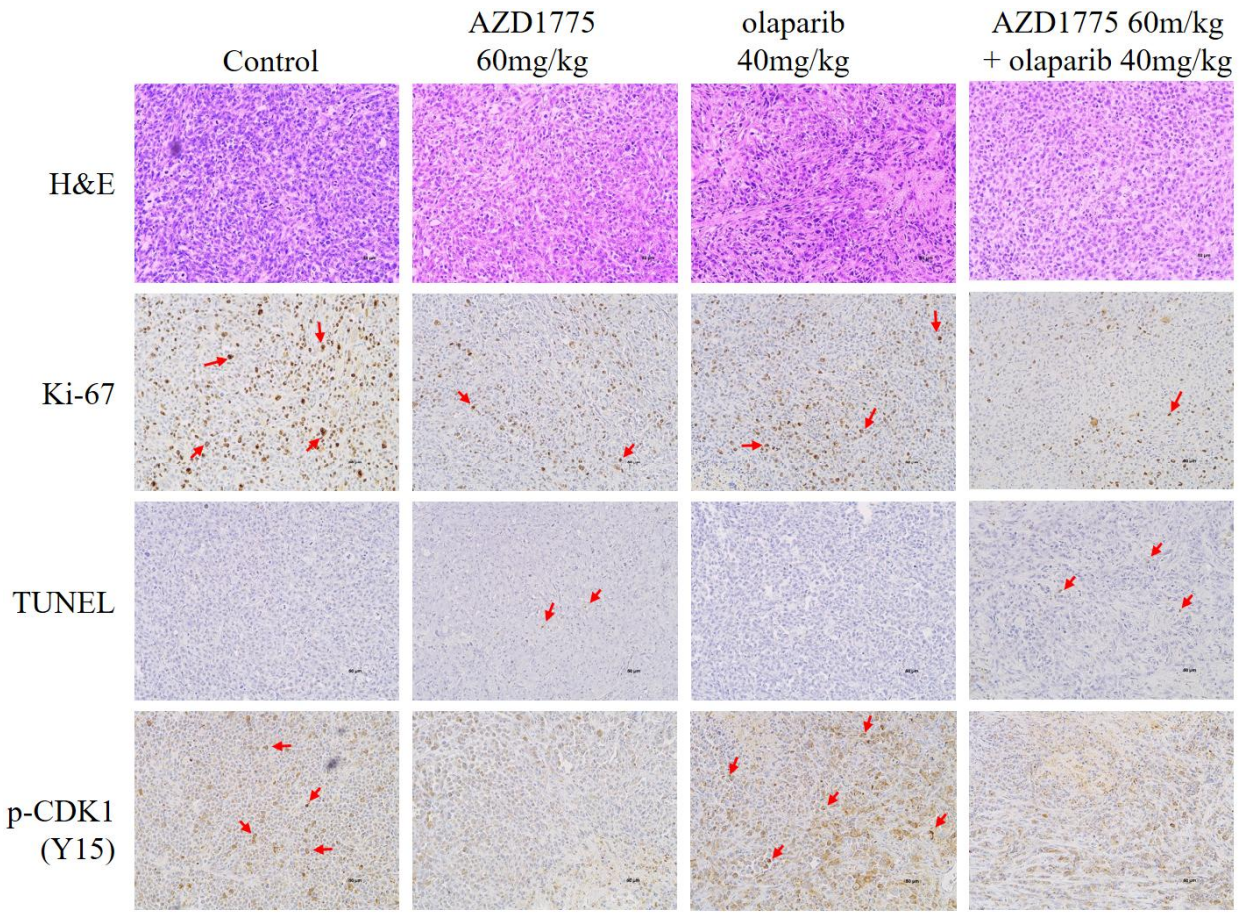
Control
AZD1775
60mg/kg
olaparib
40mg/kg
AZD1775 60m/kg
+ olaparib 40mg/kg
H&E
Ki-67
TUNEL
p-CDK1
(Y15)

Figure 26. Histological assessment of tumor response to AZD1775 alone and in combination with olaparib The tumors were removed from the mice 21 days after the drug treatment ended, and pathologic examination was done using hematoxylin and eosin (H&E) slides (x400). The scale bars represent 50μm. IHC stain for Ki-67 and TUNEL assay showed proliferation capacity and apoptosis. The kinase activity of WEE1 decreased by treatment with AZD1775 through the level of p-CDK1(Y15). The scale bars represent 50 μm. Each red arrow indicates Ki-67, TUNEL, p-CDK1(Y15).

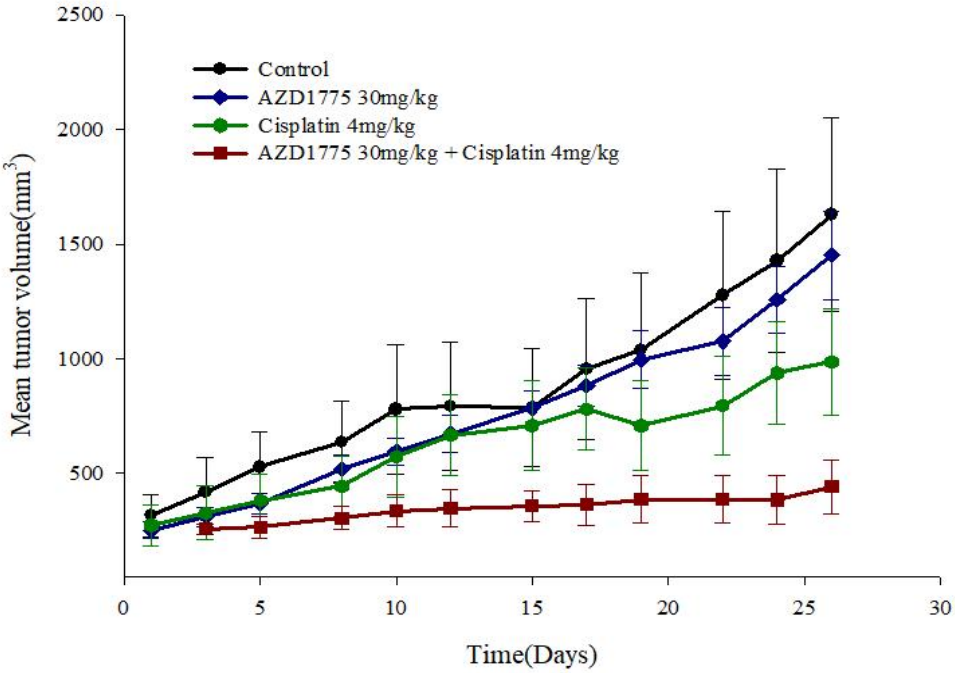
Mean tumor volume(mm3)
2500
2000
1500
1000
500
0
5
10
15
20
25
30
Time(Days)
Control
AZD1775 30mg/kg
Cisplatin 4mg/kg
AZD1775 30mg/kg + Cisplatin 4mg/kg

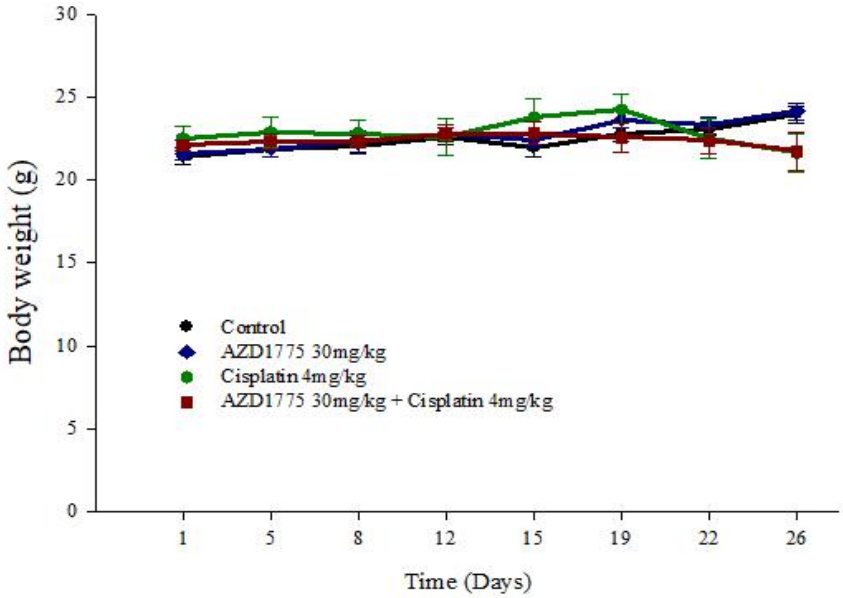
Body weight (g)
30
25
20
15
10
5
0
1
5
8
12
15
19
22
26
Time (Days)
Control
AZD1775 30mg/kg
Cisplatin 4mg/kg
AZD1775 30mg/kg + Cisplatin 4mg/kg

Figure 27. Combination treatment of cisplatin and AZD1775 showed a synergistic anti-tumor effect *in vivo* in a MDA-MB-231 xenografted mouse model.

The MDA-MB-231 human breast cancer cell line was xenografted to more than four mice per group. The mice were treated with vehicle alone, 40 mg/kg AZD1775, cisplatin 4 mg/kg and both drugs in combination. AZD1775 plus cisplatin significantly inhibited tumor growth. The toxicity of the drug was determined by measuring changes in the weight of the mouse.

Discussion

Previous studies of WEE1 inhibitors have shown that G2/M abrogation by WEE1 inhibition leads to *TP53* mutation dependent cell cytotoxicity. However, our results revealed no correlation between *TP53* mutation and AZD1775 sensitivity in TNBC cells. Some previous studies also showed that AZD1775 sensitivity was not associated with *TP53* mutation, concurrent with our findings [9-11]. We also found that WEE1 regulates the cell cycle from the S phase to mitotic exit. Sequential thymidine analog staining showed that AZD1775 accelerated S phase progression and mitotic entry (Fig. 9, 10), and that it also affected mitotic exit (Fig. 11). AZD1775 treatment inhibits the expression of spindle assembly checkpoint regulatory machinery such as BubR1 and Aurora kinase B and induces the development of multinucleated cells (Fig. 12). These features are observed in the defects of cytokinesis [23]. Indeed, there are reports that CDK1 is the main target of WEE1 inhibitor and is involved in cytokinesis [24-25]. These results suggest that WEE1 inhibition does not result in normal cytokinesis and

cell death because of increased genomic instability. In fact, when WEE1 was suppressed in a sensitive cell line, an increase in DNA content of 4n or more was observed (Fig. 11). This increase in genomic instability results in accumulation of DNA damage. We also confirmed that WEE1 inhibition decreases the level of HR related protein (Fig. 15). These results suggest that WEE1 inhibition can induce HRD by decreasing the repair ability of HR. Indeed, treatment of WEE1 inhibitor with PARP inhibitor was found to be highly effective in BRCA proficient TNBC cells. We also found that WEE1 inhibitor enhanced the sensitivity of cisplatin and ATR inhibitor. Thus, WEE1 inhibitor has great potential for use as an anti-tumor drug for treatment of TNBC.

Recent phase 2 clinical trials have shown that AZD1775 enhances the efficacy of carboplatin in patients with *TP53*-mutated ovarian cancer platinum refractory or resistant to platinum based first-line therapy [26]. In the case of ovarian cancer, BRCA mutation is known to be hypersensitive to carboplatin when compared wild type, as

indicated by overall survivals of 114 months and 71 months, respectively. In this way, when HR is intact like BRCA wild type, it is expected that there will be no response because of repair of DNA damage caused by carboplatin. However, the above clinical study of AZD1775 showed a response rate of 43% despite the inclusion of less than 10% of the BRCA mutant population. It is thought that AZD1775 increased the reactivity of carboplatin through HR modulation. Indeed, several previous studies have shown that AZD1775 increases the response to radiation [27, 28] and agents that cause DNA damage [7-9]. Our study also confirmed the effects of AZD1775 on HR capacity and revealed that AZD1775 inhibited the expression of HR machinery and disrupted DNA damage repair by inhibiting RAD51 foci formation. The inhibition of HR capacity by AZD1775 was expected to increase the reactivity of PARP inhibitors by causing phenomena such as BRCAness. Indeed, co-administration of AZD1775 and olaparib increases cytotoxicity by suppressing DNA damage response, resulting in DNA damage accumulation. Our results suggest that expansion of the HRD

phenotype expands the applicability of the PARP inhibitor, while the WEE1 inhibitor induces modulation of the HR machinery as well as cell cycle regulation, leading to DNA damage accumulation and repair attenuation.

Combined therapy with PARP inhibitor and WEE1 inhibitor can broaden the range of application of PARP inhibitor in BRCA-proficient cancers, but there is no clear mechanism for induction of HR deficiency by WEE1 inhibition. Previous reports have shown that loss of genes involved in maintenance of replication fork integrity and HR repair, such *FANCM, BRIP1, BRCA2* and *RAD50*, increases the sensitivity of the WEE1 inhibitor [29]. However, other reports have shown that WEE1 inhibition increases the inhibitory phosphorylation of BRCA2 via activity of CDK1, resulting in impaired HR [30]. Therefore, the relationship between the WEE1 and HR pathway has not been clarified. However, we showed that the anti-tumor effects of WEE1 inhibitor in TNBC cells including BRCA wildtype and *BRCA1* mutant cells varied and cell cycle regulation was different in sensitive cell lines and less sensitive cell

lines. These results indicate that WEE1 inhibitor has antitumor effects in TNBC cells, regardless of HR status.

The results of this study revealed that WEE1 inhibitor (AZD1775) increases the effects of PARP inhibitor by HR suppression in HR proficient TNBC cells. Consistent with our results, recent reports have revealed that resistance to PARP inhibitor can be overcome by WEE1 inhibition [31, 32]. Our data support that WEE1 inhibition can be applied in combination with various other DNA damage agents and DDR inhibitors, such as ATR inhibitor, via modulation of HR capacity.

In conclusion, we demonstrated the mechanism of action of AZD1775 alone and combined with olparib treatment in TNBC cells. Currently, a phase I clinical trial of combination therapy of WEE1 inhibitor (AZD1775) and PARP inhibitor (olaparib) is underway in refractory solid cancers. Our results indicate that combination treatment of PARP inhibitor and WEE1 inhibitor will help in development of clinical trial strategies for TNBC patients.

Acknowledgement

AZD1775 and olapairb were provided by AstraZeneca (Macclesfield, UK). This study was carried out through the idea and funding source of Seock-Ah Im, and and was supported by Kyung-Hun Lee, Ahrum Min, Yu-Jin Kim, Hyemin Jang, Seongyeong Kim, So Hyeon Kim, Daeun Jang, YoonJung Park.

Reference

[1] F.M. Blows, K.E. Driver, M.K. Schmidt, e. al., Subtyping of Breast Cancer by Immunohistochemistry to Investigate a Relationship between Subtype and Short and Long Term Survival: A Collaborative Analysis of Data for 10,159 Cases from 12 Studies, PLoS Medicine, 7 (2010) e1000279.

[2] V. G., Abramson, B.D. Lehmann, T.J. Ballinger, J.A. Pietenpol, Subtyping of Triple-Negative Breast Cancer: Implications for Therapy, Cancer, 121 (2015) 8-16.

[3] T.C.G.A. Network, Comprehensive molecular portraits of human breast tumours, NATURE, 490 (2012) 61-70.

[4] A. Urruticoechea, I.E. Smith, M. Dowsett, Proliferation Marker Ki-67 in Early Breast Cancer, J Clin Oncol., 23 (2005) 7212-7220.

[5] K. Do, J.H. Doroshow, S. Kummar, Wee1 kinase as a target for cancer therapy, Cell Cycle, 12 (2013) 3159-3164.

[6] A.M. Heijinka, V.A. Blomenb, X. Bisteauc, F. Degenera, F.Y. Matsushitaa, d. Philipp Kaldisc, F. Foijere, M.A.T.M.v. Vugta, A haploid genetic screen identifies the G1/S regulatory machinery as a determinant of Wee1 inhibitor sensitivity, PNAS, 112 (2015) 15160-15165.

[7] H. Hirai, Y. Iwasawa, M. Okada, T. Arai, T. Nishibata, M. Kobayashi, T. Kimura, N. Kaneko, J. Ohtani, K. Yamanaka, H. Itadani, I. Takahashi-Suzuki, K. Fukasawa, H. Oki, T. Nambu, J. Jiang, T. Sakai, H. Arakawa, T. Sakamoto, T. Sagara, T. Yoshizumi, S. Mizuarai, H. Kotani, Small-molecule inhibition of Wee1 kinase by MK-1775 selectively sensitizes p53-deficient tumor cells to DNA-damaging agents, Molecular Cancer Therapeutics, 8 (2009) 2992-3000.

[8] S. Leijen1, J.H. Beijnen, a.J.H.M. Schellens, Abrogation of the G2 Checkpoint by Inhibition of Wee-1 Kinase Results in Sensitization of p53-Deficient Tumor Cells to DNA-Damaging Agents, Current Clinical Pharmacology, 5 (2010) 186-191.

[9] A.A.V. Linden, D. Baturin, J.B. Ford, S.P. Fosmire, L. Gardner, C. Korch, P. Reigan, C.C. Porter, Inhibition of Wee1 Sensitizes Cancer Cells to Antimetabolite Chemotherapeutics In Vitro and In Vivo, Independent of p53 Functionality, Molecular Cancer Therapeutics, 12 (2013) 2675-2684.

[10] J.M. Kreahling, J.Y. Gemmer, D. Reed, D. Letson, M. Bui, S. Altiok, MK1775, A Selective Wee1 Inhibitor, Shows Single-Agent Antitumor Activity Against Sarcoma Cells, Molecular Cancer Therapeutics, 11 (2012) 174-182.

[11] A.D. Guertin, J. Li, Y. Liu, M.S. Hurd, A.G. Schuller, B. Long, H.A. Hirsch, I.

Feldman, Y. Benita, C. Toniatti, L. Zawel, S.E. Fawell, D.G. Gilliland, S.D. Shumway, Preclinical Evaluation of the WEE1 Inhibitor MK-1775 as Single-Agent Anticancer Therapy, 12, 8 (2013) 1452.

[12] M. Aarts, R. Sharpe, I. Garcia-Murillas, H. Gevensleben, M.S. Hurd, S.D. Shumway, C. Toniatti, A. Ashworth, N.C. Turner, Forced Mitotic Entry of S-Phase Cells as a Therapeutic Strategy Induced by Inhibition of WEE1, Cancer Discov, 2 (2012) 524-539.

[13] B. H, N.-K. V, L. MS, O.H. KA, P. S, H. C, M. J, G. A, N. O, S. RG, S. CS, Cyclin-dependent kinase suppression by WEE1 kinase protects the genome through control of replication initiation and nucleotide consumption., Mol Cell Biol 32 (2012) 4226-4236.

[14] R. Domínguez-Kelly, Y. Martín, S. Koundrioukoff, M.E. Tanenbaum, V.A.J. Smits, R.H. Medema, M. Debatisse, R. Freire, Wee1 controls genomic stability during replication by regulating the Mus81-Eme1 endonuclease, J Cell Biol, 194 (2011) 567-579.

[15] S.N.H. Fergus J. Couch, Priyanka Sharma, Amanda Ewart Toland, Xianshu Wang, Penelope Miron,, A.K.G. Janet E. Olson, V. Shane Pankratz, Curtis Olswold, Seth Slettedahl, Emily Hallberg,, J.I.D. Lucia Guidugli, Matthias W. Beckmann, Wolfgang Janni, Brigitte Rack, Arif B. Ekici,, I.K. Dennis J. Slamon, Florentia Fostira, Athanassios Vratimos, George Fountzilas,, W.J.T. Liisa M. Pelttari, Lorraine Durcan, Simon S. Cross, Robert Pilarski, Charles L. Shapiro,, S.Y. Jennifer Klemp, Judy Garber, Angela Cox, Hiltrud Brauch, Christine Ambrosone, Heli Nevanlinna,, S.L.S. Drakoulis Yannoukakos, Celine M. Vachon, Diana M. Eccles, and Peter A. Fasching, Inherited

Mutations in 17 Breast Cancer Susceptibility Genes Among a Large Triple-Negative Breast Cancer Cohort Unselected for Family History of Breast Cancer, J Clin Oncol., 33 (2015) 304-311.

[16] O. Amiz, M.-C. Beauchamp, P.A. Nader, I. Laskov, S. Iqbal, C.-A. Philip, A. Yasmeen, W.H. Gotlieb, Suppression of Homologous Recombination by insulin-like growth factor-1 inhibition sensitizes cancer cells to PARP inhibitors, BMC Cancer, 15 (2015).

[17] A. Min, S.-A. Im, D.K. Kim, S.-H. Song, H.-J. Kim, K.-H. Lee, T.-Y. Kim, S.-W. Han, D.-Y. Oh, T.-Y. Kim, M.J. O'connor, Y.-J. Bang, Histone deacetylase inhibitor, suberoylanilide hydroxamic acid(SAHA), enhacnes anti-tumor effects of the poly (ADP-ribose) polymerase(PARP) inhibitor olaparib in triple-negative breast cancer cells, Breast Cancer Research, 17 (2015).

[18] S. A, Yazinski, V. Comaills, R. Buisson, M.-M. Genois, H.D. Nguyen, C.K. Ho, T.T. Kwan, R. Morris, S. Lauffer, A. Nussenzweig, S. Ramaswamy, C.H. Benes, D.A. Haber, S. Maheswaran, M.J. Birrer, L. Zou, ATR inhibition disrupts rewired homologous recombination and fork protection pathways in PARP inhibitor-resistant BRCA-deficient cancer cells., Gene Dev, 31 (2017) 318-332.

[19] C. Wang, N. Jette, D. Moussienko, D.G. Bebb, S.P. Lees-Miller, ATM-Deficient Colorectal Cancer Cells Are Sensitive to the PARP Inhibitor Olaparib, Translational Oncology, 10 (2017) 190-196.

[20] T.-C. Chou, Drug combination studies and their synergy quantification using the Chou-Talalay method., Cancer Res, 70 (2010) 440-446.

[21] C. J.Matheson, D. S.Backos, PhilipReigan, Targeting WEE1 Kinase in Cancer.,

Trend in Pharmacological Sci, 37 (2016) 872-881.

[22] M.M.M. Gee, Targeting the Mitotic Catastrophe Signaling Pathway in Cancer, Mediators Inflamm, 2015 (2015).

[23] M. Kimura, T. Yoshioka1, M. Saio, Y. Banno, H. Nagaoka, Y. Okano, Mitotic catastrophe and cell death induced by depletion of centrosomal proteins, Cell Death Dis, 18 (2013) e603.

[24] I.H. Gorr, D. Boos, O. Stemmann, Mutual Inhibition of Separase and Cdk1 by Two-Step Complex Formation, Mol Cell, 19 (2005) 135-141.

[25] H. S, M. TU, Cdk1 negatively regulates midzone localization of the mitotic kinesin Mklp2 and the chromosomal passenger complex, Curr Biol, 19 (2009) 607-612.

[26] S. Leijen, R. M.J.M, v. Geel, G.S. Sonke, D.d. Jong, E.H. Rosenberg, S. Marchetti, D. Pluim, E.v. Werkhoven, S. Rose, M.A. Lee, T. Freshwater, J.H. Beijnen, J.H.M. Schellens, Phase II Study of WEE1 Inhibitor AZD1775 Plus Carboplatin in Patients With TP53-Mutated Ovarian Cancer Refractory or Resistant to First-Line Therapy Within 3 Months, J. Clin. Oncol., 34 (2016) 4354-4361.

[27] K.A. Bridges, H. Hirai, C.A. Buser, C. Brooks, H. Liu, T.A. Buchholz, J.M. Molkentine, K.A. Mason, R.E. Meyn, MK-1775, a Novel Wee1 Kinase Inhibitor, Radiosensitizes p53-Defective Human Tumor Cells, Clin Cancer Res, 17 (2011) 5638-5648.

[28] V. Caretti, L. Hiddingh, T. Lagerweij, P. Schellen, P.W. Koken, E. Hulleman, D.G.v. Vuurden, W.P. Vandertop, G.J.L. Kaspers, D.P. Noske, T. Wurdinger, WEE1 Kinase Inhibition Enhances the Radiation Response of Diffuse Intrinsic

Pontine Gliomas, Mol Cancer Ther, 12 (2013) 141-150.

[29] M. Aarts, I. Bajrami, M.T. Herrera-Abreu, R. Elliott, R. Brough, A. Asahworth, C. J.Lord, N. C.Turner, Functional Genetic Screen Identifieds Increased Sensitivity to WEE1 inhibition in Cells with Defects in Fanconi Anemia and HR pathway, Molecular Cancer Therapeutics, 14 (2015) 865-876.

[30] M. Krajewska, A. Heijink, Y. Bisselink, R. Seinstra, H. Sillje´, E.d. Vries, M.v. Vugt, Forced activation of Cdk1 via wee1 inhibition impairs homologous recombination, Oncogene, 32 (2013) 3001-3008.

[31] A. Drean, C.T. Williamson, R. Brough, I. Brandsma, M. Menon, A. Konde, I. Garcia-Murillas, H.N. Pemberton, J. Frankum, R. Rafiq, N. Badham, J. Campbell, A. Gulati, N.C. Turner, S.J. Pettitt, A. Ashworth, C.J. Lord, Modeling Therpay Resistance in BRCA1/2 Mutant Cancers, Molecular Cancer Therapeutics, 16 (2017) 2022-2034.

[32] S. Karakashev, H. Zhu, Y. Yokoyama, B. Zhao, N. Fatkhutdinov, A.V. Kossenkov, A.J. Wilson, F. Simpkins, D. Speicher, D. Khabele, B.G. Bitler, R. Zhang, BET Bromodomain Inhibition Synergizes with PARP Inhibitor in Epithelial Ovarian Cancer, Cell Reports, 21 (2017) 3398-3405.

국문 초록

WEE1 은 CDK1 의 인산화를 조절함으로써 세포주기의 G2/M checkpoint 조절에 중요한 역할을 하며 replication fork 의 안정화 및 개시에 관여를 함으로써 세포주기 전반에 관여하는 단백질이다. 또한 target 인 CDK1 의 활성의 조절은 BRCA1 의 인산화를 조절하여 DNA repair 에도 관여 하는 것으로 알려져 있다. WEE1 억제제를 처리하면 DNA replication stress 의 증가에 따라 genomic instability 가 증가하고, G/2M checkpoint 가 제 기능을 하지 못해 다양한 암 종에서 손상항암화학요법에 대한 세포 독성 효과를 향상시키는 것으로 보고되었다 .

본 연구는 삼중 음성 유방암에서 WEE1 억제제인 AZD1775 의 항종양 효과와 homologous recombination repair(상동 재조합 복구) 기전을

조절하여 DNA 손상복구 억제제인 PARP 억제제의 항종양 효과를 증가시키는 기전에 관하여 규명하고자 하였다.

AZD1775 는 약제에 감수성을 보이는 MDA-MB-231 세포 주에서 caspase-3 의존성 세포 사멸을 유도 하였고, S phase 개시의 가속화 및 세포 분열기의 조기진입을 유도 하는 등 세포주기의 비정상적 활성화를 유도하였다. 또한 AZD1775 는 DNA 손상복구 기전에 관여하는 단백질의 발현 저해 및 RAD51 foci 형성을 억제하여 상동 재조합 복구능의 저해를 유도함으로써 손상된 DNA 의 정상적인 복구가 일어나지 못하게 하였다. 이처럼 AZD1775 에 의해 저해된 DNA 손상 복구능은 PARP 억제제인 olaparib 와의 병용요법 시 유도되어지는 DNA 손상이 복구되지 못하고 축적됨으로써 세포내의 항종양효과가 증가됨을 MDA-MB-231 세포주와 동물모델에서 확인하였다.

본 연구 결과를 통해 삼중 음성 유방암에서 AZD1775 단독 혹은 olaparib 의 병용 요법의 항암 효과 가능성을 제시하며, 이러한 병용 요법에 대한 임상시험의 이론적 근거를 뒷받침 하였다.